



1 **Molecular characterization of gaseous and particulate**
2 **oxygenated compounds at a remote site in Cape Corsica in**
3 **the western Mediterranean basin.**

4 Vincent Michoud¹, Elise Hallemans^{1,2}, Laura Chiappini^{2,†}, Eva Leoz-Garziandia², Aurélie
5 Colomb³, Sébastien Dusanter⁴, Isabelle Fronval⁴, François Gheusi⁵, Jean-Luc Jaffrezo⁶,
6 Thierry Léonardis⁴, Nadine Locoge⁴, Nicolas Marchand⁷, Stéphane Sauvage⁴, Jean Sciare^{8,9},
7 Jean-François Doussin¹

8 [1] LISA, UMR CNRS 7583, Université de Paris, Université Paris-Est-Créteil, Institut Pierre Simon Laplace
9 (IPSL), Créteil, France

10 [2] Institut National de l'Environnement Industriel et des Risques, Verneuil-en-Halatte, France

11 [3] LaMP, CNRS UMR6016, Clermont Université, Université Blaise Pascal, Aubière, France

12 [4] IMT Lille Douai, Univ. Lille, SAGE - Département Sciences de l'Atmosphère et Génie de
13 l'Environnement, 59000 Lille, France

14 [5] Laboratoire d'Aérodologie, Université de Toulouse, CNRS, Toulouse, France

15 [6] Université Grenoble Alpes, CNRS, IRD, IGE, 38000 Grenoble, France

16 [7] Aix Marseille Univ, CNRS, LCE, Marseille, 13003, France

17 [8] LSCE, CNRS-CEA-UVSQ, IPSL, Université Paris-Saclay, Gif-sur-Yvette, France

18 [9] EEWRC, The Cyprus Institute, Nicosia, Cyprus

19 † deceased

20

21 **Abstract**

22 The characterization of the molecular composition of organic carbon in both gaseous and aerosol is
23 key to understand the processes involved in the formation and aging of secondary organic aerosol.
24 Therefore a technique using active sampling on cartridges and filters and derivatization followed by
25 analysis using a Thermal Desorption-Gas Chromatography/mass spectrometer (TD-GC/MS) has been
26 used to study the molecular composition of organic carbon in both gaseous and aerosol phases during
27 an intensive field campaign which took place in Corsica during the summer 2013: the ChArMEx
28 (Chemistry and Aerosol Mediterranean Experiment) SOP1b (Special Observation Period 1B) campaign.

29 These measurements led to the identification of 51 oxygenated (carbonyl and or hydroxyl) compounds
30 in the gaseous phase with concentrations comprised between 21 ng m⁻³ and 3900 ng m⁻³ and of 85
31 compounds in the particulate phase with concentrations comprised between 0.3 and 277 ng m⁻³.



1 Comparisons of these measurements with collocated data using other techniques have been
2 conducted showing fair agreement in general for most species except for glyoxal in the gas phase and
3 malonic, tartaric, malic and succinic acids in the particle phase with disagreements that can reach up
4 to a factor of 8 and 20 on average, respectively for the latter two acids.

5 Comparison between the sum of all compounds identified by TD-GC/MS in particle phase with the total
6 Organic Matter (OM) mass reveal that 18% of the total OM mass can be explained by the compounds
7 measured by TD-GC/MS for the whole campaign. This number increase to 24% of the total Water
8 Soluble OM (WSOM) measured by PILS-TOC if we consider only the sum of the soluble compounds
9 measured by TD-GC/MS. This highlights the non-negligible fraction of the OM mass identified by these
10 measurements but also the relative important fraction of OM mass remaining unidentified during the
11 campaign and therefore the complexity of characterizing exhaustively the Organic Aerosol (OA)
12 molecular chemical composition.

13 The fraction of OM measured by TD-GC/MS is largely dominated by di-carboxylic acids which
14 represents 49% of the PM_{2.5} content detected and quantified by this technique. Other contributions to
15 PM_{2.5} composition measured by TD-GC/MS are then represented by tri-carboxylic acids (15%), alcohols
16 (13%), aldehydes (10%), di-hydroxy-carboxylic acids (5%), monocarboxylic acids and ketones (3% each)
17 and hydroxyl-carboxylic acids (2%). These results highlight the importance of poly functionalized
18 carboxylic acids for OM while the chemical processes responsible for their formation in both phases
19 remain uncertain. While not measured by TD-GC/MS technique, HUmic-Like Substances (HULIS)
20 represent the most abundant identified species in the aerosol, contributing for 59% of the total
21 identified OM mass on average during the campaign.

22 14 compounds were detected and quantified in both phases allowing the calculation of experimental
23 partitioning coefficient for these species. The comparison of these experimental partitioning
24 coefficients with theoretical ones, estimated by three different models, reveals large discrepancies
25 varying from 2 to 7 orders of magnitude. These results suggest that the supposed instantaneous
26 equilibrium being established between gaseous and particulate phases assuming a homogeneous non-
27 viscous particle phase is questionable.

28

29 **1 Introduction**

30 It is now recognized that aerosols have an impact on human health, climate and ecosystems. However,
31 large uncertainties still exist on their effects, especially on climate (Fiore et al., 2015). One of the key
32 solution to reduce these uncertainties is to study the chemical composition of the aerosol organic



1 fraction since organic aerosols represent a large fraction of fine particles (Jimenez et al., 2009) which
2 impacts are compound-dependent. Molecular characterization of organic aerosol is therefore crucial.

3 The OA fraction has been widely studied (e.g. De Gouw and Jimenez, 2009; Fuzzi et al., 2006; Glasius
4 and Goldstein, 2016; Jacobson et al., 2000; Jimenez et al., 2009; Kanakidou et al., 2005; Pöschl, 2005;
5 Robinson et al., 2007; Samake et al., 2019; Seinfeld and Pankow, 2003) and many studies allowed to
6 improve our understanding of their molecular composition (e.g. Gallimore et al., 2017; Nguyen et al.,
7 2013; Nozière et al., 2015; Zhang et al., 2011b), their sources (e.g. Alves et al., 2012; Jiang et al., 2019;
8 Shrivastava et al., 2007; Woody et al., 2016), and their formation and evolution processes (e.g. Chacon-
9 Madrid and Donahue, 2011; Donahue et al., 2012; Heald et al., 2010; Li et al., 2016; Ng et al., 2011).

10 Organic aerosol can be primary or secondary. Primary Organic Aerosols (POA) are directly emitted in
11 the atmosphere, whereas Secondary Organic Aerosols (SOA) are formed after oxidation of gaseous
12 organic precursors such as Volatile Organic Compounds (VOC). These gaseous compounds, coming
13 from anthropogenic or natural sources, are progressively oxidized by atmospheric oxidants (OH, O₃
14 and NO₃). During this multigenerational oxidation process, the O/C ratio of the product formed rises
15 and their volatility decreases allowing them to condense on existing particles or to form new particles
16 through nucleation processes (Kulmala et al. 2013), leading to SOA formation. Some of the Semi-
17 Volatile Organic Compounds (SVOC) formed during the process can be split between the particulate
18 and gaseous phases. Hamilton et al. (2004) have studied the chemical composition of PM_{2.5} collected
19 in the urban atmosphere of London using a TD-GCxGC-ToF/MS (Thermal desorption- Gas
20 ChromatographyxGC-Time of Flight/ Mass Spectrometry) instrument highlighting the presence of
21 more than 10 000 different organic compounds. In the same study, 130 Oxygenated Volatile Organic
22 Compounds (OVOC) were also identified while the total number of different VOC in the atmosphere is
23 estimated to be between 10 000 and 100 000 (Goldstein and Galbally, 2007). The large number of
24 species composing the gaseous and particulate phases makes an exhaustive characterization of the
25 atmospheric organic matter challenging.

26 For this reason, analysis of principal component is often used to describe aerosol composition. This
27 type of analysis is needed to identify for example the distinction between organic fraction (OC) and
28 elemental fraction (EC) of carbonaceous particles. Aerosol Mass Spectrometer developed in the early
29 21st century (Jimenez et al., 2003) allowed making great achievements in our comprehension of aerosol
30 sources and fate leading to improved agreements between simulated and measured mass
31 concentrations. This instrument allows measuring the non-refractory fraction of PM, making up the
32 main components (NH₄⁺, NO₃⁻, SO₄²⁻, Cl⁻, organic matter (OM)) of the fine particles. However, because
33 of high fragmentation during the ionization step, molecular characterization of the organic fraction is
34 not possible. Hence, statistical methods were developed to help apportioning the results on organic



1 matter obtained with this technique. Among them, Positive Matrix Factorization (PMF) applied to
2 Aerosol Mass Spectrometer (AMS) spectra allows retrieving more information on the sources and
3 nature of organic aerosol and allows discriminating the total OA into several factors often
4 characterized by their Oxygen to carbon (O/C) ratio (e.g. Hydrocarbon like Organic Aerosol (HOA), Semi
5 volatile Oxygenated Organic Aerosol (SV-OOA), Low volatility-OOA (LV-OOA)) (Ng et al., 2010; Zhang
6 et al., 2011a). Although this classification allows getting insight into the oxidation state of OA, it is not
7 possible to identify chemical processes involved in SOA formation and aging.

8 It is therefore essential to perform molecular characterization of organic aerosol. Several techniques
9 allow this molecular characterization of OA, for example making use of off-line analyses of filter
10 samplings or online analysis following direct sampling. Coupling Particle Into Liquid Sampler (PILS) to
11 ion chromatography allow for example the measurement of organic species such as acetate, formate,
12 oxalate and methane sulfonic acid (MSA) (Orsini et al., 2003; Sciare et al., 2011). Parshintsev et al.
13 (2009) also coupled PILS with gas chromatography mass spectrometry (GC-MS), which allowed the
14 measurement of species such as alpha-pinene, pinonaldehyde, cis-pinonic and pinic acids. More
15 recently, PILS was coupled to ultra-high performance liquid chromatography and electrospray
16 ionization – quadrupole – time of flight – mass spectrometry (UPLC/ESI-Q-TOF-MS) allowing the
17 measurement of species as diverse as adenine, adonitol, sorbitol, adipic acid, vanillic acid, azelaic acid
18 cis-pinonic acid and palmitic acid (Zhang et al., 2016). Several studies also use tandem mass
19 spectrometry (MS/MS or MSⁿ) to get some structural information on compounds present in the organic
20 aerosol thanks to multiple fragmentation (e.g. Fujiwara et al., 2014; Kitanovski et al., 2011; Liu et al.,
21 2015; Nguyen et al., 2011). This technique has led to the identification of species such as carboxylic
22 acids, polycyclic aromatic hydrocarbons (PAH), oxy and nitro-PAH but also oligomers from isoprene
23 photo-oxidation experiments in the presence of low or high NO_x concentrations. Development of
24 double chromatographic systems (GCxGC or LCxLC) allows reaching lower detection limit separation
25 capacity and allows measuring a larger range of compounds (Hamilton et al., 2004; Parshintsev and
26 Hyötyläinen, 2015). Online chromatographic systems also exist to analyze the composition of the
27 particulate phase. However, difficulties in particle sampling made this type of development
28 challenging. Williams et al. (2006) developed a thermo-desorption Aerosol GC/MS-Flame Ionization
29 Detector (FID) allowing the online measurement of compounds of low polarity and with a small
30 number of chemical functions. GC analysis is usually restricted to compounds of low polarity which
31 excludes a lot of secondary component of OA. A derivatization step is therefore often used before the
32 analysis or even during the sampling to perform OA chemical characterization. For example, O-
33 (2,3,4,5,6-PentaFluoroBenzyl)HydroxylAmine (PFBHA) can be used for measurements of carbonyl
34 compounds, and N,O-bis(trimethylsilyl)-trifluoroacetamide (BSTFA) is used to reduce the polarity of



1 hydroxyl compounds (Chiappini et al., 2006; Flores and Doskey, 2015; Pietrogrande et al., 2009;
2 Schoene et al., 1994).

3 In addition of sample preparation and detection system, different types of extraction systems exist to
4 avoid multiple steps prior to analysis. For example, Chiappini et al. (2006) have developed a technique
5 using Supercritical Fluid Extraction (SFE)-GC/MS. With this technique, compounds are extracted from
6 the filter by supercritical CO₂ including a derivatization step with BSTFA as reagent inside the extraction
7 cell. Extraction efficiency depends on compound solubilities in the supercritical CO₂ which has a very
8 high solvation power. Thermo-desorption (TD) is another technique allowing to free from
9 preparation steps prior to analysis. This technique relies on the volatilization of collected compounds
10 and is suitable for semi-volatile constituent of SOA. It has the advantage to be commercially available
11 with fully automatized systems, high sensibility allowing the analysis of very low quantity of aerosol
12 and low preparation time requirement limiting the risk of lost or contamination of analyzed samples
13 (Hays and Lavrich, 2007; Parshintsev and Hyötyläinen, 2015). This technique has been used by Bates
14 et al. (2008) and van Drooge et al. (2009) to quantify particulate PAH, while Ding et al. (2009) used it
15 to measure PAH, alkanes, hopanes and steranes in PM_{2.5}.

16 Although numerous analytical methods exist for SOA chemical characterization, the multiphasic state
17 of lots of compounds is rarely studied. Indeed, gaseous phase chemical characterization is often
18 studied separately using techniques such as Proton Transfer Reaction (PTR)/MS (Hansel et al., 1995;
19 de Gouw and Warneke, 2007; Holzinger et al., 2019) or online/offline GC techniques coupled to various
20 detectors (e.g. FID, MS) (e.g. Barreira et al., 2015; Kajos et al., 2015; Valach et al., 2014). Despite this
21 disconnected treatment between aerosol and gaseous phases, understanding mechanisms controlling
22 the partitioning of SVOC between both phases is key to understand the formation and fate of SOA. A
23 partition coefficient is defined according to the thermodynamic equilibrium to calculate the mass
24 transfer of SVOC into particulate phase (Pankow, 1994). This equilibrium is thought to be dominated
25 by absorption phenomena (Liang et al., 1997) and partition coefficient is therefore calculated
26 accordingly using models. However, the validity of the instantaneous equilibrium between both phases
27 as well as the predominance of absorption processes in the mass transfer process are questionable
28 (Bateman et al., 2015; Fridlind et al., 2000; Healy et al., 2008; Rossignol et al., 2012; Virtanen et al.,
29 2010). It is therefore crucial to test the theoretical partition coefficient against values measured in the
30 field for which in situ measurements of organic compounds in both phases are needed.

31 The Mediterranean Basin is an excellent location to study organic aerosol formation and aging since it
32 experiences intensive natural and anthropogenic emissions as well as strong photochemistry (Lelieveld
33 et al., 2002). The ChArMEx project (Chemistry and Aerosols Mediterranean Experiments) aimed at
34 assessing the present and future state of the atmosphere in the Mediterranean basin. In this frame,



1 an intensive field campaign was performed at Cape Corsica for 3 weeks during summer 2013 setting
2 up numerous instruments to investigate the chemical composition of aerosol and gaseous phases.

3 As part of this project, this study aims at characterizing the molecular composition of organic carbon
4 in both the gaseous and aerosol phases during the campaign using TD-GC/MS measurements. These
5 measurements were first compared to measurements performed with other techniques (offline
6 cartridges analysis using HPLC and GC/FID-MS as well as PTR-MS for gaseous measurements and filter
7 analysis using Ion chromatography, GC/MS and HPLC). All of these measurements were used to assess
8 the composition of organic carbon and to estimate the experimental partition coefficient of
9 compounds measured in both phases to be compared with theoretical values.

10

11 **2 The ChArMEx field campaign**

12 **2.1 Description of the Cape Corse ground site**

13 The ChArMEx field campaign took place from July 15th to August 5th 2013 at Ersa in Cape Corsica
14 (42.97°N, 9.38°E) at the top of a hill (533 meters above sea level). The site is located at the northern
15 tip of a thin peninsula, a few kilometers from the sea in all directions (between 2.5 and 6 km) and
16 approximately 30 km north from the nearest urban area (Bastia). Mountains (peaking between 1000
17 and 1500 m) are limiting transport of urban air masses to the sampling site. The site is surrounded by
18 typical vegetation of Mediterranean areas (maquis shrubland). Apart from this local biogenic influence,
19 the site is mainly influenced by marine, and other natural (e.g. dust) emissions, and by continental and
20 aged air masses due to long range transport. During summer, recirculation of air masses favors
21 secondary aerosol and ozone build up (Millan et al., 1997). More details about the site, atmospheric
22 conditions encountered during the campaign and air mass origin can be found in Michoud et al. (2017).

23

24 **2.2 Sampling devices and TD-GC/MS analysis for the molecular 25 characterization of multiphase organic carbon**

26 Simultaneous sampling of gas and particulate phases has been conducted using a parallel sampling
27 system with two independent pumps allowing the selection of flow rates specifically adjusted for each
28 phase

29 Following the sampling, the molecular characterization of gaseous and particulate oxygenated organic
30 compounds sampled during the campaign has been made using a TD-GC/MS analysis after
31 derivatization steps following the method developed by Rossignol et al. (2012).

32 **2.2.1 Gaseous phase**

33 **2.2.1.1 Gaseous phase sampling**



1 Sampling of gaseous oxygenated compounds was achieved by using commercial sorbent cartridges
2 containing Tenax TA (porous polymers based on 2,6-diphenyl-p-phenylene oxide; Perkin Elmer™ or
3 Markes™) that has been previously impregnated with suitable derivatization agents (see below)
4 following an improved protocol from Rossignol et al. (2012). To maximize the adsorption surface, small
5 particle size of 60/80 mesh has been selected. Ambient air samplings were performed during 6h at a
6 flow rate of 100 mL min⁻¹. A Teflon filter (Zefluor™ membrane, Pallflex™, 47 mm) was installed
7 upstream from the cartridges to trap particulate compound that could potentially be adsorbed on
8 the Tenax adsorbent. Gaseous phase sampling has been performed using individual pumps (Gilian™
9 pump, model LFS-113DC). Prior to sampling, cartridges were heated at 320°C under a small helium
10 flow rate during 4h to eliminate any trace of contamination. Every single cartridge was then analyzed
11 to ensure its cleanliness with quantities below Limit of Detection (LOD) for all measured compounds.
12 During the campaign, 177 gaseous samples were collected following this protocol.

13 2.2.1.2 Sample preparation for gaseous phase

14 For the analysis of multi-functionalized OVOC by gas chromatography, a derivatization step is needed.
15 It allows the suppression of the reactivity of functions, improving their thermal stability and rising their
16 volatility. The dual derivatization reagents used in this study are PFBHA for carbonyl compounds and
17 MTBSTFA (N-tert-Butyldimethylsilyl-N-methyltrifluoroacetamide) for hydroxyl compounds. The two
18 derivatization processes are performed separately.

19 2.2.1.2.1 Carbonyl compounds

20 PFBHA has been used as derivatization reagent for the analysis of carbonyls. Cartridges have been
21 impregnated prior to sampling thanks to a glass balloon with 8 arms, containing 0.33mg of solid PFBHA
22 per cartridges mounted on the balloon, and on which the cartridges are installed under a 100 mL min⁻¹
23 nitrogen flow rate per cartridges at 110°C during 20 minutes. The impregnated cartridges are stored
24 at room temperature until the sampling. After sampling, cartridges are stored at room temperature
25 during 5 days, optimum for the derivatization step using PFBHA (Ho and Yu, 2002), before their
26 analysis.

27 2.2.1.2.2 Hydroxyl compounds and carboxylic acids

28 MTBSTFA with 1% of TBDMCS (tert-butyldimethylchlorosilane, used as catalyst for the reaction) has
29 been used as derivatization agent for the analysis of hydroxyl compounds. Cartridges are impregnated
30 prior to sampling vaporizing 0.3 µL of MTBSTFA at 275°C using a commercial thermal tube desorber
31 (Dynatherm Analytical Instruments, model 890) under a flow of Helium of 30 mL min⁻¹ for 11 minutes.
32 The cartridges are then stored at room temperature and sampling is performed within 10 days after
33 impregnation. After sampling, cartridges are stored at 4°C. To ensure complete derivatization of all



1 compounds before the analysis, two deposits of 0.3 μL of MTBSTFA are achieved on each side of the
2 cartridges which are kept at 60°C during 5h after that. Once the cartridges are back at room
3 temperature, analysis is performed within 5 hours.

4 **2.2.2 Particulate phase**

5 2.2.2.1 Particulate phase sampling

6 Sampling of particulate matter was performed over regular (not impregnated) filters and derivatization
7 was performed only after sampling (to avoid chemisorption of gaseous compounds on filters) following
8 a protocol adapted from Rossignol et al. (2012). The sampling device used during the campaign was a
9 modified Speciation Sampler Partisol, model 2300 (Rupprecht & Patashnick Co, Thermo Fisher
10 Scientific). Three ChemComb cartridges, with $\text{PM}_{2.5}$ impactors, were mounted to this device to allow
11 the sampling of particulate phase on filters of different nature according to targeted compounds. For
12 carbonyls compounds and non-oxygenated compounds Quartz filters (Pallflex™, 47 mm) were used.
13 For hydroxyl compounds, quartz filters are not suitable because of silanol groups present at their
14 surfaces that can be derivatized instead of the hydroxyl compounds reducing considerably their
15 derivatization yield (Rossignol, 2012). Therefore, for the sampling of this type of compounds, we
16 selected filters of borosilicate glass fibers coated with tetrafluoroethylene (TFE) called hereafter
17 “Teflon quartz filters” (Fiber film, Pallflex™, 47mm). Activated carbon honeycomb denuders were
18 installed upstream from the filters to avoid positive artifacts due to adsorption of gaseous oxygenated
19 compounds on the filters. For cleaning and a best efficiency, denuders were heated at 250°C before
20 being used for each new sample. The sampling flow rate was of 1 $\text{m}^3 \text{h}^{-1}$ for each sample step. Quartz
21 and Teflon quartz filters were carbonized prior to the sampling respectively at 500°C and 300°C to
22 eliminate any possible contamination. During the campaign, 240 particulate samples were collected
23 following this protocol.

24 2.2.2.2 Sample preparation for particulate phase

25 2.2.2.2.1 Carbonyl compounds

26 Sampling are performed on quartz filters which are stored at -16°C after sampling waiting for analysis.
27 Then, the filters are cut into two pieces, both inserted into empty and clean stainless steel tubes. These
28 tubes, including grids, are previously sonicated in several bath of ultra-pure water and acetonitrile and
29 then are heated at 400°C under a flow of helium (80 mL min^{-1}) during 4h. Deposition of 50 μL of PFBHA
30 saturated solution (acetonitrile/water (90/10, v/v) with 27 mg mL^{-1} of PFBHA) are achieved in the tubes
31 to expose adsorbed compounds to the derivatization reagent. Tubes are then stored at room
32 temperature during 5 days to allow derivatization of adsorbed compounds before their analysis.

33 2.2.2.2.2 Hydroxyl compounds and carboxylic acids



1 Sampling are performed on Teflon quartz filters which are stored at -16°C after sampling waiting for
2 analysis. Derivatization is performed after sampling directly on filters. Filters are put in stainless steel
3 tubes cleaned following the same protocol than for carbonyl compounds. Tubes are then sealed and
4 maintained vertically with 10 μl of MTBSTFA put in the bottom cap for passive impregnation during
5 24h at room temperature.

6 **2.3.3 Analytical system**

7 The analytical system used in this study is composed by three successive modules: a thermal
8 desorption system, a gas chromatography unit and a mass spectrometer.

9 The thermal desorption allows the extraction of adsorbed compounds on sample support by increasing
10 the temperature without any preliminary solvent extraction and collecting them on a cold trap before
11 flash injection in GC/MS instrument. The thermal desorption system (Markes™, model unity 1) is
12 coupled with an automated system (Markes™, model Ultra 50:50). Thermal desorption parameters are
13 listed in Table 1.

14 The GC/MS instrument (Agilent Technologies Inc.) used during this study is composed by two modules:

- 15 - A GC unit, model 6890 A, associated with a capillary column Integra-Guard Rxi®-5Sil MS
16 (stationary phase: 1.4-bis(dimethylsiloxy)phenylene dimethyl polysiloxane, length: 60m,
17 diameter: 250 μm , film thickness: 0.25 μm , with 5m pre-column deactivated without any
18 stationary phase; Restek Corporation).
- 19 - A Mass spectrometer, model 5973N, equipped with an ionization source in EI (Electronic
20 Impact) or CI (Chemical Ionization; using CH_4 as reagent gas) and associated with a quadrupole.

21 GC/MS parameters are listed in Table 1.

22 **2.3.4 Internal calibration protocol**

23 For a more efficient quantification, internal calibration has been set up for both family of compounds
24 (carbonyl and hydroxyl) and for both phases. This procedure aims at taking into account drift in MS
25 sensitivity and derivatization efficiency. Two types of internal standards are used: substitutes which
26 are deuterated compounds getting at least one derivatized function; and an internal standard which is
27 a compound with no derivatized function. 50 ng of Substitutes are added prior to the derivatization
28 step to take into account every steps of sample preparation as well as analysis steps. The list of
29 substitutes selected is given in Table 2. The internal standard selected is pentadecane and 50 ng is
30 added on cartridges grid just before the analysis.

31 **2.3.5 Estimation of uncertainties**



1 Overall uncertainties have been determined taking into account precision, detection limit and
2 systematic errors (including uncertainties on standard concentrations, on calibration, on blank
3 determination and on sampling volume; following Gaussian error propagation). Overall uncertainties
4 have therefore been estimated to be 35% and 54% on averaged in gas phase for carbonyls and
5 hydroxyls and carboxylic acids respectively and to be 41% and 47% on averaged in particulate phase
6 for carbonyls and hydroxyls and carboxylic acids respectively.

7 **2.4 Ancillary measurements**

8 An important set of complementary instruments, dedicated to the measurement of both gaseous and
9 particulate phase, has been deployed at the supersite supporting the interpretation and validation of
10 the TD-GC/MS dataset.

11 **2.4.1 Gaseous ancillary measurements**

12 **2.4.1.1 PTR-MS**

13 Measurements of OVOCs (e.g. nopinone, sum of methacrolein and methyl vinyl ketone, propanoic acid
14 and methyl ethyl ketone), among other species (e.g. aromatics and biogenic VOCs) were performed
15 using a Proton Transfer Reaction-Time of Flight Mass Spectrometer (PTR-ToF-MS, KORE Inc® 2nd
16 generation). A detailed description of these measurements was given by Michoud et al. (2017, 2018).
17 Briefly, ambient air was sampled through a 5-m long Teflon PFA (PerFluoroAlkoxy) line held at 50°C at a
18 flow rate of 1.2 L min⁻¹, leading to a residence time of 3.1s in the sampling line. The PTR-ToF-MS
19 sampling flow rate was set at 150 mL min⁻¹. The instrument was operated at a reactor pressure and a
20 temperature of 1.33 mbar and 40°C, respectively, leading to an E/N ratio of 135 Td.

21 An automated zero procedure was performed every hour for 10 min. Humid zero air was generated by
22 passing ambient air through a catalytic converter to perform zeros at the same relative humidity than
23 ambient air.

24 Signals from protonated VOCs were normalized by the signals of H₃O⁺ and the first water cluster
25 H₃O⁺(H₂O) as proposed by de Gouw and Warneke (2007). Concentrations were calculated using Eq. (1):

$$[R] = \frac{i_{R_net}}{(i_{H_3O^+} + X_r \cdot i_{H_3O^+(H_2O)})} \cdot \frac{150000}{R_{f,R}} \quad (1)$$

26 Where [R] represents the mixing ratio of a given VOC, i_{R_net} the net signal of this VOC, $i_{H_3O^+}$ and $i_{H_3O^+(H_2O)}$
27 the signals of H₃O⁺ and H₃O⁺(H₂O). X_r is a factor introduced to account for the effect of humidity on the
28 PTR-MS sensitivity (de Gouw and Warneke, 2007) and is determined experimentally through
29 calibrations performed at various relative humidity. $R_{f,R}$ is the sensitivity determined during calibration
30 experiments (in ncts ppt⁻¹) and normalized to 150 000 counts s⁻¹ of H₃O⁺ ions. The latter is the number



1 of counts of reagent ions (not corrected for ion transmission into the ToFMS) observed on this PTR-
2 ToF-MS instrument. Data were recorded at a time resolution of 1 min. During the campaign,
3 calibrations were performed every 3 days using various standards, including a canister containing 15
4 VOCs (NMHCs, OVOCs and chlorinated VOCs; Restek®), a gas cylinder containing 9 NMHCs (Praxair®)
5 and a gas cylinder containing 9 OVOCs (Praxair®). Information about the composition of these
6 standards can be found in Michoud et al. (2017). Overall uncertainties are estimated between 6 and
7 23% depending on the compound considered (Michoud et al., 2017) following the “Aerosols, Clouds,
8 and Trace gases Research InfraStructure network” (ACTRIS) guidelines for uncertainty evaluation
9 (ACTRIS, 2012).

10 2.4.1.2 GC-FID/MS

11 OVOCs, including aldehydes, ketones, alcohols, ethers, esters, as well as a few NMHCs, including BVOCs
12 and aromatics, were measured using an online GC/FID-MS instrument. This instrument as well as its
13 setup during the campaign was described by Michoud et al. (2017). Briefly, ambient air was sampled
14 via a KI ozone scrubber and a 5-m long PFA line (1/8”) at a flow rate of 15 mL min⁻¹ using an Air server-
15 unity I (Markes International®). The sample was pre-diluted (50% dilution) with dry zero air to keep
16 relative humidity below 50%. The sample was then collected in an internal trap, consisting in a 1.9 mm
17 i.d. quartz tube filled with two different sorbents (5 mg of Carbopack B and 75 mg of Carbopack X,
18 Supelco®) and cooled at 12.5 °C by a Peltier system. Compounds trapped on the sorbents were then
19 thermally desorbed at 280 °C and injected into the column of a GC (Agilent®) equipped with a FID for
20 detection and quantification and with a Mass Spectrometer (MS) for identification. The compounds
21 were separated through a high polar CP-lowox column (30 m×0.53 mm× 10 µm) (Varian®). The time
22 resolution of these measurements is 1h30min. Calibrations were performed during the campaign using
23 a gas cylinder containing 29 VOCs (Praxair). Information about the composition of this standard can be
24 found in Michoud et al. (2017). Overall uncertainties are estimated between 5 and 14% depending on
25 the compound considered (Michoud et al., 2017) following ACTRIS guidelines for uncertainty
26 evaluation (ACTRIS, 2012).

27 2.4.1.3 Active sampling on DNPH cartridges

28 Carbonyl compounds were collected continuously for 3 h durations by active sampling on DNPH
29 cartridges (Waters®) using an automatic sampler (Tera Environment®). These compounds were
30 analyzed later by High Performance Liquid Chromatography (HPLC) with UV detection. Ambient air was
31 sampled via a 3-m PFA line (1/4”) at 1.5 L min⁻¹ and passed through a KI ozone scrubber and a stainless-
32 steel particle filter (porosity: 2µm). More details about these measurements are given by Michoud et
33 al. (2017; 2018). Calibrations were performed at the laboratory using Supelco® standard for DNPH.



1 Overall uncertainties are estimated around 25% (Michoud et al., 2017) following ACTRIS guidelines for
2 uncertainty evaluation (ACTRIS, 2012).

3 2.4.1.4 Inorganic trace gases

4 During the campaign, NO and NO₂ were measured by a commercial ozone chemiluminescence analyzer
5 (Cranox II; Eco Physics®) with a time resolution of 5 min. NO was measured directly, while NO₂ was
6 converted into NO using a photolytic converter. O₃ was measured using a commercial analyzer (TEI 49i;
7 Thermo Environmental Instruments Inc®) using UV absorption with a time resolution of 5 min.

8 **2.4.2 Particulate ancillary measurements**

9 Mass concentrations of PM₁₀ and PM₁ were measured during the campaign using two tapered element
10 oscillating microbalance (TEOM) equipped with a filter dynamic measurement system (FDMS) (Thermo
11 Scientific™). In addition, aerosol chemical composition was measured by online technique (aerosol
12 chemical speciation monitor - ACSM) and offline-method (Ion chromatography, GC/MS and HPLC) on
13 filters collected daily with 2 HiVol samplers (30 m³ hr⁻¹) equipped with PM₁ and PM_{2.5} inlets.

14 2.4.2.2 ACSM

15 Measurements of the chemical composition of non-refractory submicron aerosol (NR-PM₁) have been
16 carried out using a quadrupole ACSM (Aerodyne Research Inc., Billerica, MA, USA). These
17 measurements have been described in detail by Michoud et al. (2017). Briefly, the calibration of this
18 instrument with monodispersed (300 nm diameter) ammonium nitrate particles was performed 2
19 months before the campaign. Because ambient air was dried by a Nafion membrane and because
20 ammonium nitrate was low during the campaign, constant collection efficiency (CE) of 0.5 has been
21 kept. The Q-ACSM was operated continuously during the whole campaign at a time resolution of 30
22 min.

23 2.4.2.3 Ion Chromatography

24 Soluble anions and cations were analyzed by ionic chromatography (IC, ThermoFisher ICS3000)
25 following protocol similar to that described elsewhere (e.g. Jaffrezo et al., 1998). Briefly, 38 mm
26 diameter sub-samples from each filter were soaked for 20 min in 10 mL of Milli-Q water with orbital
27 shaking, and then filtered using 0,22 µm-porosity Acrodisc filters before analysis. ASA11-HC and CS16
28 columns were used for anions and cations analyses, respectively.

29 2.4.2.4 GC/MS

30 Organic markers were analyzed by gas chromatography (GC) coupled with mass spectrometry (MS)
31 using the method developed by El Haddad et al. (2011). Filter samples were first spiked with 300µL of
32 a solution containing the internal standard D6-Cholesterol (C₂₄H₄₀D₆₀). Accelerated Solvent Extraction



1 (ASE Dionex 300) was performed with a mixture of acetone/dichloromethane (1/1 v/v) at 100bar and
2 100°C during 10 min. Sample extracts were concentrated using a Turbo Vap II under N₂ in a water-bath
3 regulated at 40°C to a final volume of 500µL. A fraction of the extracts (50µL) was derivatized at 70°C
4 for 90 min by adding 100µL of N,O-bis(triméthylsilyl)trifluoroacétamide (BSTFA containing 1% of
5 TMCS). Derivatized extracts were then analyzed using a Thermo Trace Ultra GC coupled with a Polaris
6 Q – ion trap operating in the electron impact mode. The GC was equipped with a TR-5MS capillary
7 column (30 m × 0.25 mm i.d. × 0.25 µm film thickness). Aliquots of 1 µL were injected in split mode
8 (split ratio 50) at 280°C. The column temperature program was held at 65°C hold for 2 min, and ramped
9 at 6°C/min up to 300°C, followed by an isothermal hold at 300°C for 20 min. GC-MS response factors
10 were determined using authentic standards. Compounds, for which no authentic standard are
11 available, were quantified using the response factor of compounds with analogous chemical
12 structures. Field blank filters were also treated with the same procedure.

13 2.4.2.5 HPLC

14 The analysis of a large array of organic acids (including pinic and phthalic acids, and 3-MBTCA) was
15 conducted using the same water extracts as for IC and HPLC-PAD analyses. In brief, this was performed
16 by HPLC-MS (GP40 Dionex with a LCQ-FLEET Thermo-Fisher ion trap), with negative mode
17 electrospray ionization. The separation column is a Synergi 4 µm Fusion – RP 80A (250×3 mm ID, 4 µm
18 particle size, from Phenomenex). An elution gradient was optimized for the separation of the
19 compounds, with a binary solvent gradient consisting of 0.1% formic acid in acetonitrile (solvent A)
20 and 0.1% aqueous formic acid (solvent B) in various proportions during the 40-minute analytical run.
21 Column temperature was maintained to 30 °C. Eluent flow rate was 0.5 ml min⁻¹, and injection volume
22 was 250 µl. Calibrations were performed for each analytical batch with solutions of authentic
23 standards. All standards and samples were spiked with internal standards (phthalic-3,4,5,6-d4 acid and
24 succinic-2,2,3,3-d4 acid). The calculation of the final atmospheric concentrations was corrected with
25 the concentrations of internal standards and of the procedural blanks, taking also into account the
26 extraction efficiency varying between 76-116% (depending on the acid).

27 2.4.2.6 OCEC SUNSET field instrument

28 Concentrations of elemental carbon (EC) and organic carbon (OC) in PM_{2.5} were obtained in the field
29 from an OCEC Sunset field instrument (Sunset Laboratory, Forest Grove, OR, USA; Bae et al., 2004)
30 operated at a flow rate of 8 L min⁻¹ with a denuder set upstream to avoid adsorption of semi-volatile
31 compounds on the filter collecting particles in the instrument. Data were obtained every 2 hours with
32 this instrument.

33 2.4.2.7 PILS-TOC



1 PM₁ water-soluble organic compounds (WSOCs) were measured by a modified PILS (Brechtel
2 Manufacturing Inc., USA; Sorooshian et al., 2006) coupled with an analyzer of total organic carbon
3 (TOC; model Sievers 900; Ionics Ltd, USA). Sciare et al. (2011) and Michoud et al. (2017) described this
4 technique and operating procedures used during the ChArMEx field campaign. Briefly, the PILS-TOC
5 instrument was operated at a flow rate of 15 L min⁻¹ with a dilution factor of 1.30. A 0.45 μm pore size
6 diameter filter in polyethylene was set in-line in the aerosol liquid flow to analyze the water-soluble
7 OC fraction only and a VOC denuder was set upstream the collection to avoid semi-volatile VOC
8 contamination. Daily blanks were conducted every day for 1h by placing a total filter upstream of the
9 sampling system.

10 2.4.2.8 HULIS measurements

11 The water soluble HULIS fraction is analyzed according to a protocol described in detail in Baduel et al.
12 (2009). Briefly, the water-soluble fractions obtained from aerosol samples are passed through a weak
13 anion exchange resin (GE Healthcare[®], HiTrap™ DEAE FF, 0.7cm ID x 2.5cm length) without any pre-
14 treatment. After this concentration step, the organic matter adsorbed is washed with 12mL of a
15 solution of NaOH 0.04M (J.T.Baker[®], pro analysis) to remove neutral components, hydrophobic bases,
16 inorganic anion, mono- and di-acids initially retained in the resin. Finally, HULIS_{WS} are quickly eluted in
17 a single broad peak using 4 mL of a high ionic strength solution of NaCl 1M (Normapur[®]). All flow rates
18 are set at 1.0 mL min⁻¹. UV-Vis absorption spectra are measured on-line after the extraction system,
19 using a diode array detector (Dionex UV-VIS 340U), and recorded in the range 220-550nm. The HULIS_{WS}
20 fraction is subsequently collected manually and the carbon content is analyzed with a DOC analyser
21 (Shimadzu TOC-V_{CPH/CPN}) by catalytic burning at 680°C in oxygen followed by non-dispersive infrared
22 detection of the evolved CO₂.

23

24 3 Results and discussion

25 3.1 Main conditions during the campaign

26 3.1.1 Meteorological conditions

27 Meteorological and environmental conditions are presented in Table 3. Relatively high temperatures
28 were monitored during the campaign (up to 32°C) coinciding with high biogenic emissions from local
29 vegetation and strong photochemistry (Michoud et al., 2017). These conditions led to high ozone
30 concentrations during the campaign (65 ppbv on average for the overall sampling period and up to 111
31 ppbv for 5 min measurements), typical of this region during summer (e.g. Lelieveld, 2002; Di Biagio et
32 al., 2015). High relative humidity was encountered at night with values reaching 100% coinciding with
33 foggy conditions observed during several nights at the site. High wind speeds were monitored with
34 maximum reached on the 30th of July 2013 (13.2 m s⁻¹). During the campaign, almost 40% of air masses



1 came from the south-west sector and 20% from the western sector (see Figure 1). Winds coming from
2 south-west sector are predominant during daytime and nighttime and correspond to wind speed
3 maxima. Winds from the west and north-east are also recorded, but during daytime only. Low NO_x
4 concentrations were observed during the campaign (0.57 ppbv on average) with a few spikes above 1
5 ppbv corresponding to local influence from traffic especially when air masses came from the south
6 (e.g. 27th July).

7 **3.1.2 Particles and organic fraction**

8 Mean, median, maximum and minimum of mass concentrations of PM₁₀, PM₁ and organic fraction in
9 NR-PM₁ are summarized in Table 3 for the whole campaign. The averaged mass concentrations for
10 PM₁₀ is 12.0 µg m⁻³, comparable to observations performed at other remote sites located in the
11 western Mediterranean basin (e.g. 15.5 µg m⁻³ at Montseny, Spain; 11.5 µg m⁻³ between 2010 and
12 2013 at Montsec, Spain; 14.6 µg m⁻³ at Monte Martano, Italy; 13 µg m⁻³ between 2010 and 2013 at
13 Venaco, France – Moroni et al., 2015; Nicolas, 2013; Querol et al., 2009a, 2009b; Ripoll et al., 2015).
14 The averaged mass concentrations for PM₁ was 8.3 µg m⁻³ during the campaign and represented an
15 important fraction of PM₁₀ (69% on average). The amount of PM₁ at Erza is also comparable to what
16 has been previously measured in other remote sites in the western Mediterranean basin (e.g. 8.2 µg
17 m⁻³ at Montseny, Spain; 7.1 µg m⁻³ between 2010 and 2013 at Montsec, Spain – Minguillón et al., 2015;
18 Ripoll et al., 2015). During the campaign, the organic fraction represented between 40 and 55% of PM₁
19 mass concentrations (mean of 3.7 µg m⁻³ representing 44% of PM₁ on average).

20 Time series of mass concentrations of PM₁₀, PM₁ and organic fraction in PM₁ are presented in Figure
21 2. Highest mass concentrations for PM₁₀ and PM₁ are observed between 12 and 21 July (15.7 and
22 11.0 µg m⁻³ on average respectively for PM₁₀ and PM₁). According to back trajectory analysis (Michoud
23 et al., 2017) this period corresponds to low wind speed and hence stationary air masses. A decrease of
24 PM₁₀ concentrations is observed from 21 to 25 July (12.0 µg m⁻³ on average) while the ratio PM₁/PM₁₀
25 and organic/PM₁ are the highest. During this period, the PM₁₀ and PM₁ fractions are almost the same.
26 This period is characterized by higher wind speed and air masses coming from the north-eastern sector
27 and therefore characterized by anthropogenic influence from northern Italy. From 26 to 29 July, a rise
28 in PM₁₀ mass concentrations is observed coinciding with the warmest temperature of the campaign
29 and air masses coming from the south and characterized by biogenic influence (see Michoud et al.,
30 2017). From 29 July to 3 August, PM₁ concentrations strongly decrease (from 9.3 to 2.6 µg m⁻³ on
31 average) coinciding with higher wind speed and relative humidity while winds came from north-west
32 and north-east directions (see Michoud et al. 2017). During the last period (3-5 August), increase of
33 PM₁₀ and PM₁ concentrations is observed and a clear diurnal cycle is monitored for both fractions



1 corresponding to a raise in temperatures. Overall, the organic fraction evolution follows the one of the
2 PM_{10} mass fraction.

3 **3.2 Results from the TD-GC/MS analysis**

4 **3.2.1 Compound identifications**

5 Detection of functionalized compounds led to the identification of 23 carbonyl compounds and 28
6 hydroxyl compounds and carboxylic acids in the gaseous phase and of 30 carbonyl compounds and 55
7 hydroxyl compounds and carboxylic acids in the particulate phase. The entire list of these 97
8 compounds is presented in supplementary material 1 together with their O/C ratio, their calculated
9 saturation vapor pressure, the main fragments of their mass spectra, the method used for their
10 identification, the substitute used to account for the derivatization efficiency, the external standard
11 used for their quantification, the fragment used for quantification and the averaged concentrations
12 measured in both phases. For the carbonyl compounds, the mono-functionalized compounds
13 identified contained from 3 (e.g. propanal) to 10 (e.g. decanal) carbon atoms and from 2 (e.g. glyoxal)
14 to 5 (e.g. 4-oxopentanal) carbon atoms for the bi-functionalized compounds. For the hydroxyl
15 compounds and the carboxylic acids, the mono-functionalized identified compounds contained from
16 3 (e.g. propanoic acid) to 18 (e.g. octadecanoic acid) carbon atoms. Several poly-functionalized
17 compounds have also been identified: hydroxy-acids and di-acids from 2 (e.g. glycolic acid) to 8 (e.g.
18 mandelic acid) carbon atoms; triols, di-hydroxy-acids, hydroxyl-di-acids, tri-acids from 3 (e.g. glycerol)
19 to 9 (e.g. 2-Hydroxy-4-isopropyl-hexanedioic acid) carbon atoms; and two tetra-functionalized
20 compounds (methyl-tetrols and citric acid).

21 It is worth noting that several compounds exhibited very close quantities in the air sample and in the
22 blank (designed as "blank" in the supplementary material 1). Therefore, the presence of these
23 compounds in the air sampled cannot be certain. For the compounds that have been quantified
24 successfully and present concentrations significantly above the quantification limit (3σ above averaged
25 blank measurements), higher levels are observed in the gas phase. The averaged concentrations
26 ranged from 21 $ng\ m^{-3}$ (Mandelic acid) to 1600 $ng\ m^{-3}$ (glycerol) for hydroxyl compounds in the gas
27 phase and from 0.3 (Pyruvic acid) to 277 (oxalic acid) $ng\ m^{-3}$ in the particulate phase. For the carbonyl
28 compounds, the averaged concentrations ranged from 85 $ng\ m^{-3}$ (hexanone) to 3900 $ng\ m^{-3}$ (4-
29 Oxopentanal) in the gas phase and from 1 $ng\ m^{-3}$ (e.g. methylpropanal or glyoxal) to 20 $ng\ m^{-3}$ (4-
30 methylpentanal) in the particulate phase. Figure 3 presents the distribution of all quantified
31 compounds along their saturation vapor pressure and their O/C ratio. The phases in which these
32 compounds were identified are also shown in Figure 3. While compounds only present in the gas or
33 aerosol phase exhibit high and low saturation vapor pressure, respectively, some exceptions are
34 noticeable. Indeed, some gaseous compounds have low vapor pressure (down to $10^{-8.6}$ atm) such as



1 long chain linear mono carboxylic acids (up to 15 carbon atoms) and some compounds only found in
2 the particle phase have high vapor pressure (up to $10^{-0.8}$ atm), normally incompatible with their
3 presence in such phase, such as small mono carbonyls (e.g. methylpropanal, methylbutanone, 2-
4 methylbutanal...). We also found compounds exhibiting high vapor pressure (up to $10^{-0.4}$ atm) in both
5 phases, which is normally incompatible with their presence in aerosol phase, such as small carbonyls
6 (e.g. propanal, acrolein, methacrolein, MVK...). This latest point is discussed further in section 3.2.5.

7 **3.2.2 Data intercomparison**

8 A comparison of data measured by TD-GC/MS with other techniques available on site has been
9 performed, for both phases, to test the reliability of these measurements.

10 3.2.2.1 Gas phase

11 Comparisons of TD-GC/MS data with PTR-ToF-MS and GC/FID/MS data averaged over the same
12 sampling duration at a similar time step have been performed and are shown in Figure 4 and Figure 5.
13 Fair agreement is found for nopinone, the sum of methacrolein and methyl vinyl ketone, propanoic
14 acid and methyl ethyl ketone between TD-GC/MS measurements and measurements performed by
15 PTR-ToF-MS. Good agreement is also found for methyl vinyl ketone and 2-hexanone between TD-
16 GC/MS measurements and measurements performed by GC/FID/MS. Ranges of measured
17 concentrations are similar between these techniques as well as the temporal variation.

18 Comparisons of TD-GC/MS measurements with DNPH cartridges analysis are presented in Figure 6. For
19 these latter, only the first ten days of the campaign have been validated because of a leak issue in the
20 sampling system of DNPH cartridges after that period (see Michoud et al., 2017). Ranges of
21 concentrations are in the same order of magnitude between these two techniques for propanal,
22 acrolein, methacrolein, methyl ethyl ketone, methylglyoxal, hexanal and benzaldehyde even though it
23 is difficult to conclude on their co-variation regarding the small number of data available and the low
24 time resolution for these two techniques. However, glyoxal and methyl vinyl ketone present large
25 differences between the two techniques (factor of 15 and 12 respectively). For glyoxal, Matsunaga
26 (2004) recorded maximum concentrations of 154 ng m^{-3} ($\approx 65 \text{ pptv}$) at a forested site at Moshiri in
27 Hokkaido island, in summer. Washenfelder et al. (2011) recorded maximum glyoxal concentrations of
28 500 pptv at an urban site in Los Angeles in summer, while numerous glyoxal precursors exist in urban
29 environment. Therefore, the concentrations measured by TD-GC/MS seem overestimated and
30 measurements from DNPH cartridges analysis seem more consistent with these previous observations.
31 Thermo-degradation of other heavier compounds adsorbed on the Tenax cartridges leading to glyoxal
32 could be an hypothesis for this overestimation. In the case of methyl vinyl ketone, the good agreement
33 observed between TD-GC/MS measurements and GC/FID/MS ones (see Figure 5) tends to indicate that



1 the disagreement observed here is related to an underestimation of the concentrations measured by
2 DNPH cartridge analysis. Furthermore, recent studies on humidity dependence of the DNPH–HPLC–UV
3 method for some ketone compounds, revealed that the collection efficiency is inversely related to
4 relative humidity, with up to 35 %–80 % of the ketones being lost for RH values higher than 50 % at
5 22 °C (Ho et al., 2014). Furthermore, dimerization issues for MVK during analyses using DNPH method
6 has also been identified, during more recent measurements, that can cause strong underestimation of
7 this technique (>50%).

8 3.2.2.2 Particulate phase

9 Comparisons of results from filter analysis by TD-GC/MS and by Ion chromatography, GC/MS and HPLC
10 have been performed and are shown in Figure 7 and Figure 8. The range of concentrations between
11 TD-GC/MS analysis and other techniques are in the same order of magnitude for oxalic acid, pinic acid,
12 2-methylglyceric acid, MBTCA, glycolic acid and phthalic acid. However, a discrepancy is found for
13 malonic acid and tartaric acid which measurements differ both of a factor of 4 on averaged between
14 TD-GC/MS and HPLC analyses. For methyl-tetrols, the analysis performed by TD-GC/MS did not allow
15 to distinguish the two isomers. Temporal evolution of compounds shown in Figure 7 and Figure 8 are
16 also similar from one technique to another, especially for oxalic acid and pinic acid.

17 Nevertheless, larger disagreements have been observed for some compounds (see Figure 8). An
18 overestimation of TD-GC/MS analysis compared to HPLC analysis of a factor of 8 and 20 on average,
19 respectively for malic acid and succinic acid, is observed. For malic acid, the external standard used for
20 the estimation of the response factor (glycolic acid) is maybe not appropriate which may explain this
21 discrepancy. As a test, succinic acid and glutaric acid (two other di-acids) have been used as external
22 standard for malic acid quantification with no improvement in the agreement observed. For succinic
23 acid, the authentic standard has been used and such problem cannot explain the discrepancy
24 observed. No interference in the peak region is observed and this cannot neither explain the
25 differences observed.

26 On the whole, comparisons of TD-GC/MS with other techniques deployed during the campaign are
27 satisfactory for both phases with results at least in the same order of magnitude for the measured
28 absolute concentrations, except for some compounds. Therefore, these observations allow us to use
29 TD-GC/MS data both in gas and aerosol phase to study further the behavior of organic carbon at a
30 molecular level at cape Corsica during ChArMEx campaign, keeping however in mind the potential
31 biases revealed during this data comparison exercise.

32 3.2.3 Description of organic compounds behaviour during the campaign



1 Time series of every compounds measured by TD-GC/MS in both phases are presented in the
2 supplementary material 2.

3 Concerning the gaseous phase, several linear mono-aldehydes (C_3 to C_{10}) have been detected and
4 quantified in the same range of concentrations than what has been previously reported by the same
5 technique at another site in Corsica (Rossignol et al., 2016). These compounds are mainly primary
6 compounds emitted by vegetation under stress conditions. For propanal and butanal, some chemical
7 processes and anthropogenic primary sources (especially ship emission) can also be involved (Agrawal
8 et al., 2008). During the campaign, these compounds are characterized by daily maxima during daytime
9 and daily minima during nighttime, confirming the predominance of biogenic sources. This diurnal
10 cycle is also found when these compounds are also measured in the particulate phase, which may
11 indicate a thermodynamic equilibrium for these compounds between both phases. Their
12 concentrations are higher at the end of the campaign (30th of July) coinciding with the warmest period
13 suggesting higher local biogenic emission.

14 At the end of the campaign, an elevation of concentrations is also observed for nopinone, 4-
15 oxopentanal, 2-propenoic acid, methacrylic acid, mandelic acid, glycolic acid and levulinic acid (see
16 supplementary material 2), all known as oxidation products of biogenic compounds. For example,
17 Nopinone is an oxidation product of beta-pinene and 4-oxopentanal is known to be an oxidation
18 product of several biogenic compounds such as squalene and limonene (Fruekilde et al., 1998;
19 Matsunaga et al., 2004; Rossignol et al., 2012). During this period, air masses were coming from the
20 southern sector and travelled during a short period of time (12 to 24h) above Corsica and Sardinia
21 (Michoud et al., 2017; Zannoni et al., 2017). An increase of concentrations is also observed for some
22 monocarboxylic acids such as propanoic acid, pentanoic acid, hexanoic acid, tridecanoic acid,
23 tetradecanoic acid and pentadecanoic acid (see supplementary material 2). Several sources are
24 possible for these compounds that can be either primary or secondary and either biogenic or
25 anthropogenic, especially for small carboxylic acids (C_3 to C_6 ; Chebbi and Carlier, 1996). Longer chain
26 carboxylic acids are often considered as primary compounds both from biogenic and anthropogenic
27 sources. Nevertheless, the results we obtained here underline the ubiquitous nature of organic acids
28 (including long chains) in the atmosphere. It is remarkable to observe that despite their widespread
29 detection, the knowledge on their sources (including chemical processes) remain scarce. Ozonolysis of
30 alkenes, reactions between aldehydes and HO_2 , or hydrolysis of oligomers could be involved.

31 At the beginning of the campaign (from 13th to 15th July) we observed a rise in concentrations of 4-
32 oxopentanal, 2-hexanone, glycolic acid, 2-propenoic acid and monocarboxylic acids from C_3 to C_7 ((see
33 supplementary material 2). A spike of methacrolein is also observed the 13th of July, highlighting local
34 emission of biogenic precursors as it is during the calm low wind cluster period (Michoud et al, 2017).



1 Concerning particulate compounds, observations are different than for gaseous compounds. Indeed,
2 an important peak of concentrations is observed for many compounds from 17th to 19th of July, e.g. 3-
3 isopropylglutaric acid, 3-hydroxy-4,4-dimethylglutaric acid, ketonorlimonic acid, ketolimonic acid,
4 tricarballic acid and methyltartronic acid (see supplementary material 2). The four first compounds
5 correspond to oxidation products of biogenic precursors such as pinenes and limonene. O/C ratios for
6 these compounds are high, varying from 0.5 (3-isopropylglutaric acid) to 1.3 (methyltartronic acid).
7 This period corresponds to a rise in aerosol mass concentration (see Figure 2), with stagnant air masses
8 and very low wind speed (Michoud et al., 2017). Associated with strong photochemistry, this favored
9 chemical processing and the formation of secondary products with high O/C ratio. Other compounds
10 also show a rise in their concentrations at this time (see supplementary material 2): unsaturated
11 carboxylic acids (crotonic acid, 2-hydroxy-3methyl-2-pentenoic acid), long-chain monocarboxylic acids
12 (hexadecanoic acid and octadecanoic acid), dicarboxylic acids (malonic acid, succinic acid, glutaric
13 acid), unsaturated dicarboxylic acids (maleic acid, fumaric acid, 3-methyl-2-pentenedioic acid),
14 erythrose (a triol compound), 2,3-dihydroxypropanoic acid (a dihydroxy acid), hydroxy-diacids (2-
15 hydroglutaric acid, 2-hydroxy-4-isopropylhexandioic acid, 3-hydroxy-2-pentenedioic acid, 3-hydroxy-
16 3-methylglutaric acid, 3-hydroxyhexandioic acid, malic acid) and also 2-MGA, 3-MBTCA and DHOPA.

17 Higher concentrations for DHOPA, 2-MGA, MBTCA, and HGA are observed from 20 to 24 July (see
18 supplementary material 2). 2-MGA is formed, in presence of NO_x (Ding et al., 2014, Fu et al., 2009;
19 Giorio et al., 2017), through the oxidation of methacrolein and methacrylic acid, both oxidation
20 products of isoprene. This period is characterized by the highest NO_x concentrations of the campaign
21 (averaged concentrations of 1 ppbv against 0.6 ppbv for the rest of the campaign). Some dicarboxylic
22 acids (e.g. malonic acid, succinic acid and glutaric acid) also show a rise in their concentrations during
23 this period. This suggest a strong photochemical activity with an important aging of the air masses
24 collected and an advanced photochemical age for this period, also characterized by high OH missing
25 reactivity observed at the site (Zannoni et al., 2017). On the contrary, from the 27th of July to the end
26 of the campaign, levels of concentrations for these compounds decrease (see supplementary material
27 2) suggesting less aged air masses. This is also revealed by the higher (cis-pinonic acid + pinic
28 acid)/MBTCA ratio observed during this last period (see supplementary material 2). Indeed, this ratio
29 allows the evaluation of the oxidation state of air masses since cis-pinonic acid and pinic acid are first
30 generation oxidation products of monoterpenes while MBTCA is known to be a higher generation
31 oxidation product (Ding et al., 2014).

32 Observations of MSA (methanesulfonic acid, CH₃SO₃H) and water soluble HULIS are reported in
33 supplementary material S3. MSA is an oxidation product of dimethyl sulfide (DMS), a gaseous
34 compound emitted by marine phytoplankton activity, and is mostly present in particulate phase. MSA



1 can therefore be used to identify influence of marine chemistry on aerosol composition. Higher MSA
2 concentrations are observed on 23 to 28 July and on 4 August when air masses were coming from the
3 west sectors and spent days above sea (see Michoud et al., 2017) and on the first period of the
4 campaign (15-18 July) when air masses were stagnant with very low wind speed (see Michoud et al.,
5 2017). In summer, HULIS are mostly formed through secondary oligomerization processes in the
6 particulate phase (Baduel et al., 2010). Higher water soluble HULIS concentrations are observed on 20-
7 21 July when air masses are originating from north-east sector bringing continental aged air-masses
8 (Michoud et al., 2017) and on 27 July when air masses were coming from the southern sector with
9 large biogenic influence (Michoud et al. 2017). This is consistent with the formation of HULIS through
10 secondary oligomerization processes in summer from both anthropogenic and biogenic precursors
11 (Srivastava et al., 2018).

12 **3.2.4 Molecular characterization of particulate matter**

13 A time series of total mass quantified by TD-GC/MS in PM_{2.5} is presented in Figure 9. This sum has been
14 calculated using the QL/2 (quantification limit/2) value when data were below the limit of
15 quantification. The sum of all the compounds measured by TD-GC/MS represents an average of
16 630 ng m⁻³ for the whole campaign with a minimum of 54 ng m⁻³ and a maximum of 2400 ng m⁻³
17 measured on the 17th of July.

18 This sum is also compared to the organic matter mass concentration in PM_{2.5} (see Figure 9). OM is
19 calculated using the organic carbon (OC) concentration measured by the SUNSET field instrument with
20 a ratio between OC and OM of 1.9 for Cape Corsica as proposed by Michoud et al. (2017). On average
21 18% of the total OM mass can be explained by the compounds measured by TD-GC/MS for the whole
22 campaign. From 12 to 29 July, oxygenated compounds measured by TD-GC/MS represent more than
23 20% on average of measured OM while they represented less than 10% between July 29 and August
24 4. If measured water soluble HULIS are added to these compounds, analysed compounds represent
25 36% of measured OM on averaged and up to 100% on 16 July.

26 Some of the compounds identified and quantified by TD-GC/MS, especially carboxylic acids, are soluble
27 in aqueous phase. To allow a comparison between TD-GC/MS measurement and WSOC (Water Soluble
28 Organic Carbon) measurements conducted by PILS-TOC, only soluble compounds measured by TD-
29 GC/MS have been selected (see Figure 10). Indeed, we considered only the compounds having a
30 Henry's law constant higher than 10⁴ M atm⁻¹. For every compounds measured by TD-GC/MS, the
31 Henry's law constants have been determined by the Structure Activity Relationship (SAR) developed
32 by Raventos-Duran et al. (2010) using the online platform of GECKO-A model (Aumont et al., 2005;
33 http://geckoa.lisa.u-pec.fr/generateur_form.php). At the end, 39 different compounds have been
34 selected for the calculation of this sum and no aldehyde or ketone were kept in this selection.



1 Comparing the sums of compounds measured by TD-GC/MS considering only soluble ones or
2 considering all of them reveals very similar behaviors and level of concentrations (see Figure 10). On
3 average, soluble compounds represent 72% of the total concentration of PM measured by TD-GC/MS
4 despite the important number of compounds not considered as soluble (26 compounds over 58 not
5 considered). Time series of soluble compounds measured by TD-GC/MS and of WSOM have similar
6 behaviors with higher concentrations during the period comprised between 17 and 23 July and smaller
7 concentrations at the end of the campaign. It is worth noting that WSOM corresponds to PM₁ while
8 TD-GC/MS measurements concern PM_{2.5}. On average, the sum of the soluble compounds measured by
9 TD-GC/MS represented 24% of the total WSOM measured by PILS-TOC. If measured water soluble
10 HULIS are added to these soluble compounds, analysed water soluble compounds represent 58% of
11 measured WSOM on averaged and up to 100% on 15 and 17 July.

12 Time series and average composition of the PM_{2.5} measured by TD-GC/MS are presented respectively
13 in Figure 11 and Figure 12. Almost half of the PM_{2.5} measured by TD-GC/MS are characterized by di-
14 carboxylic acid (49%) with oxalic acid being the most important by far. Other contributors to PM_{2.5}
15 composition measured by TD-GC/MS are tri-carboxylic acids (15%), alcohols (13%), aldehydes (10%),
16 di-hydroxy-carboxylic acids (5%), monocarboxylic acids and ketones (3% each) and hydroxyl-carboxylic
17 acids (2%). High concentrations of di-carboxylic acids are observed from 13 to 28 July (441 ng m⁻³ on
18 average; 51% of the total OM measured by TD-GC/MS). After the 29th of July, the contribution of di-
19 carboxylic acids decreases significantly to reach 30%. The end of the campaign is characterized by
20 intense fresh local biogenic emissions leading to less processed air masses and OM composed mostly
21 by mono-functionalized compounds. On a general basis, organic acids constitute the principal
22 contributors to the fraction of organic aerosol measured by TD-GC/MS during this campaign while only
23 few chemical processes are known to lead to their formation (see section 3.2.3). The identification of
24 many di-carboxylic acids implies the existence of unknown chemical processes both in gaseous phase
25 and even more probably in particulate phase to explain their formation (Hammes et al., 2019). These
26 missing processes in chemical mechanism included in models might contribute to their inability to
27 reproduce correctly the formation and aging of SOA. If HULIS are considered in this analysis, they
28 represent 59% of the total identified OM mass on average, ranging from 21% of contribution at the
29 beginning of the campaign to more than 80% at the end of the campaign (from 31 July to 3 August).

30 **3.2.5 Partitioning of organic carbon between gaseous and particulate phases**

31 Many of the compounds identified during the campaign are present in both the gas and aerosol phases.
32 The partitioning coefficient is therefore key to understand processes governing the equilibrium
33 between both phases. For the compounds present in both phases, an experimental partitioning
34 coefficient can be determined following eq. 2 relying on the Pankow equilibrium.



$$K_{pe,i} = \frac{F_i/TSP}{A_i} \quad (2)$$

1 $K_{pe,i}$ corresponds to the experimental partitioning coefficient for the compounds i , F_i corresponds to
2 the concentration in the particulate phase, A_i corresponds to the concentration in gaseous phase and
3 TSP (Total Suspended Particulate matter) corresponds to the total mass concentration of particles
4 measured by TEOM-FDMS ($\mu\text{g m}^{-3}$). Uncertainties for experimental partitioning coefficients take into
5 account uncertainties on the measurement of concentrations in both phases (see section 2.3.5) and
6 on the TEOM measurement (estimated to be 25%).

7 Further, another expression of the Pankow equilibrium allows for the determination of theoretical
8 partitioning coefficients using eq. 3.

$$K_{pt,i} = \frac{760RTf_{om}}{MW_{om}\zeta_i 10^6 p_{L,i}^0} \quad (3)$$

9 $K_{pt,i}$ corresponds to the theoretical partitioning coefficient for the compounds i , R to the ideal gas
10 constant, T to the temperature in Kelvin, f_{om} to the OM mass fraction, MW_{om} to the averaged molar
11 mass of compounds constituting organic particulate matter (g mol^{-1}), ζ_i to the activity coefficient, $p_{L,i}^0$
12 to the saturation vapor pressure (Torr). Saturation vapor pressures have been determined at 295K
13 (averaged temperature of the campaign) using three different models (Moller et al., 2008; Myrdal and
14 Yalkowsky, 1997; Nannoolal et al., 2008). f_{om} has been set to 0.8 using the averaged OC/TC ratio
15 measured by the SUNSET field instrument.

16 Experimental (averaged over the campaign) and theoretical partitioning coefficients obtained for
17 compounds identified in both phases are presented in Table 4 and Figure 13 and are compared to
18 experimental coefficient obtained in a previous field study in Corsica and a chamber study in the
19 EUPHORE simulation chamber (Rossignol et al., 2016). For most of the compounds, experimental
20 partitioning coefficients obtained for the three campaigns are relatively close to each other, with some
21 differences that can however reach up to an order of magnitude (e.g. dimethylglyoxal or acrolein, even
22 two orders of magnitude for glyoxal). These observed differences are small compared to the
23 differences recorded between experimental and theoretical coefficients, with an observed
24 underestimation of theoretical coefficients varying from 1 to 7 orders of magnitude. It is worth noting
25 that the three models used for theoretical coefficients determination are in good agreement. Higher
26 differences between experimental and theoretical coefficients are observed for hydroxyl compounds
27 and carboxylic acids with a shift of the equilibrium toward the particulate phase for experimental
28 partitioning coefficients. It is worth noting that a denuder is used upstream the filter collection to avoid
29 overestimation of particulate organic matter due to adsorption of semi-volatile compounds onto the



1 filter, therefore excluding potential positive artefact for concentrations of compounds in particulate
2 phase that could have led to overestimation of experimental partitioning coefficients. Furthermore,
3 underestimation of gaseous concentrations for these compounds in such high proportion is unlikely,
4 especially when we look at the comparisons performed for OVOCs with other measurement
5 techniques (see section 3.2.2.1).

6 The differences observed between experimental and theoretical partitioning coefficient may be
7 explained by the high humidity conditions encountered during the campaign (mean RH value of 70%,
8 see Table 3). Indeed, theoretical partitioning coefficient as described by the Pankow equilibrium does
9 not take into account the presence of an aqueous phase or a deliquescent aerosol, while, soluble
10 organic compounds can split between gaseous, aqueous and particulate phase. Concerning the
11 partitioning between the gaseous and aqueous phases, the Henry law's constant and the activity
12 coefficients are considered to calculate the thermodynamic equilibrium.

13 These differences could also be explained by the fact that the equilibrium between both phases is not
14 reached. This could be due to the viscosity of particles. Some studies showed that organic aerosol can
15 be found in various states, from liquid to semi-solid (viscous) (Bateman et al., 2016; Booth et al., 2014,
16 Shiraiwa et al., 2011; Virtanen et al., 2010). The viscosity of the particle can limit the diffusion inside
17 the particle, which can lead to an inhomogeneity in the composition with the formation of a gradient
18 of concentrations between the surface and the center of the particle (Chan et al., 2014; Davies and
19 Wilson, 2015; Zobrist et al., 2011). The equilibrium could therefore only concern an external layer of
20 the particle and the gaseous phase (Davies and Wilson, 2015); or on the contrary a semi-solid external
21 layer, caused by the aging of the particle, could prevent the equilibrium to settle between the
22 particulate bulk and the gaseous phase.

23 Furthermore, Soonsin et al. (2010) showed that the physical state of the particle can influence the
24 activity coefficient of some compounds and especially of dicarboxylic acids. Partitioning coefficients
25 are calculated considering a liquid phase for aerosols. Considering a solid or semi-solid phase for
26 aerosols would lead to a decrease in the vapor pressure estimation for such compounds and therefore
27 to higher theoretical partitioning coefficients.

28 In addition, polymerization and oligomerization processes in the particulate phase have been
29 highlighted in previous studies through the identification of compounds with high masses (Hallquist et
30 al., 2009; Kalberer et al., 2004; Lim et al., 2010; Tolocka et al., 2004). The formation of oligomers
31 increases the viscosity of the particle during its aging (Abramson et al., 2013). These reactions could
32 also explain the presence of semi-volatile compounds in the particulate phase in such high proportion,
33 especially for carbonyls that have high vapor pressure and which should not be detected in the aerosol



1 phase based on the theory. Indeed, numerous studies reveal the possibility of formation of oligomers,
2 inside the particle, from carbonyls such as α -di-carbonyls, for example glyoxal or methylglyoxal (Gao
3 et al., 2004a, 2004b; Hastings et al., 2005; Iinuma et al., 2004; Jang et al., 2002, 2003; Jang and Kamens,
4 2001; Liggio et al., 2005a, 2005b; Lim et al., 2010; Tolocka et al., 2004). These reactions are favored
5 under low water content in the particles. On the contrary, under higher humidity conditions, oligomers
6 can form back monomer compounds which in case of viscous particle can be trapped into the
7 particulate phase. It is worth noting that higher experimental partitioning coefficients are found for
8 most compounds on 20 July and 26-27 July while water soluble HULIS concentrations are at their
9 maximum. HULIS are known to be formed through secondary oligomerization processes in summer
10 (Baduel et al., 2010), supporting the hypothesis that these kind of processes might be partly
11 responsible for the disagreement between experimental and theoretical partitioning coefficient.

12 Even if an analytical artifact cannot be ruled out, for example a fragmentation of oligomers to form
13 back the monomer compounds during the analysis, numerous evidences support the experimental
14 results presented here and suggest that the instantaneous equilibrium being established between
15 gaseous and particulate phases assuming a homogeneous non-viscous particle phase is not fully
16 representative of the real atmosphere.

17 **Conclusion**

18 A multiphasic molecular characterization of oxygenated compounds has been carried out during the
19 ChArMEx SOP 1b field campaign held in Erba Corsica during July 2013 using an analytical technique
20 based on multi-support sampling (filters and adsorbent containing cartridges), derivatization
21 procedure and TD-GC/MS analysis. The deployment of this analytical technique in the field allows the
22 identification of 97 different compounds in the gas (24 different compounds) and aerosol (50 different
23 compounds) phases, some of them being present in both phases (23 different compounds). These
24 compounds include simple carbonyls, alcohols or carboxylic acids as well as multi-functional
25 compounds up to four functional groups. Among all the quantified compounds, the important
26 contribution of organic acids (67% of the organic aerosol concentration measured by TD-GC/MS)
27 emphasizes the existence of unknown chemical processes both in the gaseous phase and even more
28 probably in the particulate phase to explain their formation. The absence of such processes in chemical
29 mechanisms may contribute to the inability of models to correctly reproduce the formation and aging
30 of SOA.

31 Comparisons of these measurements with other measurements performed at the site when available
32 reveal fair agreement on the whole for almost all compounds experiencing redundant measurement
33 in both phase with concentrations at least in the same order of magnitude. Noticeable disagreements



1 (larger than a factor of 8 and up to a factor of 15) have however been found for glyoxal in the gas phase
2 between TD-GC/MS measurements and DNPH cartridges analysis and for malic and succinic acid in the
3 particulate phase between TD-GC/MS measurements and HPLC analysis. Nevertheless, comparisons
4 of TD-GC/MS with other techniques deployed during the campaign are in general agreement,
5 validating their use to conduct further analysis.

6 While the data obtained are very valuable to provide additional insight into the composition of organic
7 matter for air masses encountered during the campaign, it is worth noting that it represents only a
8 fraction of the total mass of organic matter. Indeed, an attempt to close the mass budget of organic
9 aerosol using the TD-GC/MS measurements reveal that the sum of all particulate oxygenated organic
10 compounds measured by this technique account for 18% of the total OM mass on average for the
11 whole campaign. This portion of OM identified at the molecular scale is not constant and mostly
12 depends on the oxidation state of the sampled air masses. If we only consider the soluble compounds
13 measured by TD-GC/MS, they represent 24% of the total WSOM on average. Therefore, a sizeable
14 fraction of the OM mass was identified by TD-GC/MS analysis, but a very large fraction of OM mass
15 remained unidentified during the campaign, highlighting the complexity of an exhaustive
16 characterization of the OA chemical composition at the molecular scale. An important fraction of this
17 unidentified OM mass is due to HULIS.

18 Finally, for the compounds quantified in both the gas and the aerosol phases, a comparison between
19 experimental and theoretical partitioning coefficients has been performed revealing in most cases a
20 large underestimation by the theory reaching 1 to 7 orders of magnitude. It indicates that the
21 partitioning theory is most often inappropriate, since it is based on the instantaneous equilibrium
22 being established between gaseous and particulate phases, assuming a homogeneous non-viscous
23 particle phase, which is the base for aerosol modeling. Furthermore, the partitioning of semi-volatile
24 compounds is influenced by meteorological conditions (humidity, temperature) and inherent
25 properties of particles (viscosity, water content, organic fraction concentrations, acidity, etc.). In
26 addition, the way these conditions impact the partitioning of semi-volatile compounds strongly
27 depends on the physico-chemical properties of the considered compounds (solubility, saturation vapor
28 pressure, reactivity, etc.).

29

30 **Data availability.**

31 Access to the data used for this publication is restricted to registered users following the data and
32 publication policy of the ChArMEx program ([http://mistrals.sedoo.fr/ChArMEx/](http://mistrals.sedoo.fr/ChArMEx/Data-Policy/ChArMEx_DataPolicy.pdf) Data-
33 Policy/ChArMEx_DataPolicy.pdf).



1

2 **Author contributions.**

3 VM and EH participated in the field campaign and prepared the paper with inputs from all co-authors.
4 LC, ELG and JFD were involved in TD-GC/MS measurements and supervised this work. SD, IF, TL, NL
5 and SS participated in the field campaign and were in charge of VOC measurements (GC-FID/MS, PTR-
6 MS, Active sampling on DNPH cartridges). AC and FG were in charge of inorganic trace gases
7 measurements (NO_x and O₃). JS participated in the field campaign and was in charge of aerosol
8 measurements by ACSM, OCEC instrument, PILS-TOC and IC. JLJ and NM were in charge of aerosol
9 speciation measurements during the campaign through filter analysis (IC, GC/MS, HPLC, HULIS
10 measurements).

11

12 **Competing interests.**

13 The authors declare that they have no conflict of interest.

14

15 **Special issue statement.**

16 This article is part of the special issue “CHemistry and AeRosols Mediterranean EXperiments (ChArMEx;
17 ACP/AMT inter-journal SI)”. It does not belong to a conference.

18

19 **Acknowledgements.**

20 This study received financial support from the MISTRALS and ChArMEx programs, ADEME, the French
21 Environmental Ministry, and the Communauté Territoriale de Corse (CORSiCA project). This project
22 was also supported by the CaPPA project (Chemical and Physical Properties of the Atmosphere),
23 funded by the French National Research Agency (ANR) through the PIA (Programme d’Investissement
24 d’Avenir) under contract ANR-11-LABX-0005- 01 and by the Regional Council Nord-Pas de Calais and
25 the European Funds for Regional Economic Development (FEDER).

26 The authors also want to thank Eric Hamonou and François Dulac for logistical help during the
27 campaign and all the participants of the ChArMEx SOP1b field campaign. This paper is dedicated to the
28 memory of our friend and colleague Laura Chiappini, who passed away shortly after the campaign.
29 Laura conceived the original idea for this work and created the conditions to have this experimental
30 worked done. Analyses at IGE were performed on the Air O Sol platform partly funded with the Labex
31 OSUG@2020 (ANR10 LABX56)



1 References

- 2 Abramson, E., Imre, D., Beránek, J., Wilson, J. and Zelenyuk, A.: Experimental determination of
3 chemical diffusion within secondary organic aerosol particles, *Phys. Chem. Chem. Phys.*, 15(8), 2983–
4 2991, doi:10.1039/C2CP44013J, 2013.
- 5 ACTRIS: Measurement Guideline VOC: WP4- NA4: Trace gases networking: Volatile organic carbon
6 and nitrogen oxides Deliverable D4.1: Draft for standardized operating procedures (SOPs) for VOC
7 measurements, 25–30, http://www.actris.net/Portals/97/deliverables/PU/WP4_D4.1_M12_v2.pdf
8 (last access: 21 July 2020), 2012.
- 9 Agrawal, H., Welch, W. A., Miller, J. W. and Cocker, D. R.: Emission Measurements from a Crude Oil
10 Tanker at Sea, *Environ. Sci. Technol.*, 42(19), 7098–7103, doi:10.1021/es703102y, 2008.
- 11 Alves, C., Vicente, A., Pio, C., Kiss, G., Hoffer, A., Decesari, S., Prevôt, A. S. H., Minguillón, M. C.,
12 Querol, X., Hillamo, R., Spindler, G. and Swietlicki, E.: Organic compounds in aerosols from selected
13 European sites – biogenic versus anthropogenic sources, *Atmos. Environ.*, 59, 243–255,
14 doi:10.1016/j.atmosenv.2012.06.013, 2012.
- 15 Aumont, B., Szopa, S. and Madronich, S.: Modelling the evolution of organic carbon during its gas-
16 phase tropospheric oxidation: development of an explicit model based on a self generating approach,
17 *Atmos Chem Phys*, 5(9), 2497–2517, doi:10.5194/acp-5-2497-2005, 2005.
- 18 Baduel, C., Voisin, D., and Jaffrezo, J. L.: Comparison of analytical methods for Humic Like Substances
19 (HULIS) measurements in atmospheric particles, *Atmos. Chem. Phys.*, 9, 5949–5962,
20 <https://doi.org/10.5194/acp-9-5949-2009>, 2009.
- 21 Baduel, C., Voisin, D., and Jaffrezo, J.-L.: Seasonal variations of concentrations and optical properties
22 of water soluble HULIS collected in urban environments, *Atmos. Chem. Phys.*, 10, 4085–4095,
23 <https://doi.org/10.5194/acp-10-4085-2010>, 2010.
- 24 Bae, M.-S., Schauer, J. J., DeMinter, J. T., Turner, J. R., Smith, D., and Cary, R. A.: Validation of a semi-
25 continuous instrument for elemental carbon and organic carbon using a thermal-optical method,
26 *Atmos. Environ.*, 38, 2885–2893, 2004.
- 27 Barreira, L. M. F., Parshintsev, J., Kärkkäinen, N., Hartonen, K., Jussila, M., Kajos, M., Kulmala, M. and
28 Riekkola, M.-L.: Field measurements of biogenic volatile organic compounds in the atmosphere by
29 dynamic solid-phase microextraction and portable gas chromatography-mass spectrometry, *Atmos.*
30 *Environ.*, 115, 214–222, doi:10.1016/j.atmosenv.2015.05.064, 2015.
- 31 Bateman, A. P., Bertram, A. K. and Martin, S. T.: Hygroscopic influence on the semisolid-to-liquid
32 transition of secondary organic materials, *J. Phys. Chem. A*, 119(19), 4386–4395,
33 doi:10.1021/jp508521c, 2015.
- 34 Bateman, A. P., Gong, Z., Liu, P., Sato, B., Cirino, G., Zhang, Y., Artaxo, P., Bertram, A. K., Manzi, A. O.,
35 Rizzo, L. V., Souza, R. A. F., Zaveri, R. A. and Martin, S. T.: Sub-micrometre particulate matter is
36 primarily in liquid form over Amazon rainforest, *Nat. Geosci.*, 9(1), 34–37, doi:10.1038/ngeo2599,
37 2016.
- 38 Bates, M., Bruno, P., Caputi, M., Caselli, M., de Gennaro, G. and Tutino, M.: Analysis of polycyclic
39 aromatic hydrocarbons (PAHs) in airborne particles by direct sample introduction thermal desorption
40 GC/MS, *Atmos. Environ.*, 42(24), 6144–6151, doi:10.1016/j.atmosenv.2008.03.050, 2008.



- 1 Booth, A. M., Murphy, B., Riipinen, I., Percival, C. J. and Topping, D. O.: Connecting bulk viscosity
2 measurements to kinetic limitations on attaining equilibrium for a model aerosol composition,
3 *Environ. Sci. Technol.*, 48(16), 9298–9305, doi:10.1021/es501705c, 2014.
- 4 Chacon-Madrid, H. J. and Donahue, N. M.: Fragmentation vs. functionalization : chemical aging and
5 organic aerosol formation, *Atmospheric Chem. Phys.*, 11(20), 10553–10563, doi:10.5194/acp-11-
6 10553-2011, 2011.
- 7 Chan, M. N., Zhang, H., Goldstein, A. H. and Wilson, K. R.: Role of Water and Phase in the
8 Heterogeneous Oxidation of Solid and Aqueous Succinic Acid Aerosol by Hydroxyl Radicals, *J. Phys.*
9 *Chem. C*, 118(50), 28978–28992, doi:10.1021/jp5012022, 2014.
- 10 Chebbi, A. and Carlier, P.: Carboxylic acids in the troposphere, occurrence, sources, and sinks: A
11 review, *Atmos. Environ.*, 30(24), 4233–4249, doi:10.1016/1352-2310(96)00102-1, 1996.
- 12 Chiappini, L., Perraudin, E., Durand-Jolibois, R. and Doussin, J. F.: Development of a supercritical fluid
13 extraction–gas chromatography–mass spectrometry method for the identification of highly polar
14 compounds in secondary organic aerosols formed from biogenic hydrocarbons in smog chamber
15 experiments, *Anal. Bioanal. Chem.*, 386(6), 1749–1759, doi:10.1007/s00216-006-0744-3, 2006.
- 16 Davies, J. F. and Wilson, K. R.: Nanoscale interfacial gradients formed by the reactive uptake of OH
17 radicals onto viscous aerosol surfaces, *Chem Sci*, 6(12), 7020–7027, doi:10.1039/C5SC02326B, 2015.
- 18 De Gouw, J. and Jimenez, J. L.: Organic Aerosols in the Earth’s Atmosphere, *Environ. Sci. Technol.*,
19 43(20), 7614–7618, doi:10.1021/es9006004, 2009.
- 20 de Gouw, J. and Warneke, C.: Measurements of volatile organic compounds in the earth’s
21 atmosphere using proton-transferreaction mass spectrometry, *Mass. Spectrom. Rev.*, 26, 223–257,
22 doi:10.1002/mas.20119, 2007.
- 23 Di Biagio, C., Doppler, L., Gaimoz, C., Grand, N., Ancellet, G., Raut, J.-C., Beekmann, M., Borbon, A.,
24 Sartelet, K., Attié, J.-L., Ravetta, F. and Formenti, P.: Continental pollution in the western
25 Mediterranean basin: vertical profiles of aerosol and trace gases measured over the sea during
26 TRAQA 2012 and SAFMED 2013, *Atmos Chem Phys*, 15(16), 9611–9630, doi:10.5194/acp-15-9611-
27 2015, 2015.
- 28 Ding, X., He, Q.-F., Shen, R.-Q., Yu, Q.-Q. and Wang, X.-M.: Spatial distributions of secondary organic
29 aerosols from isoprene, monoterpenes, β -caryophyllene, and aromatics over China during summer, *J.*
30 *Geophys. Res. Atmospheres*, 119(20), 2014JD021748, doi:10.1002/2014JD021748, 2014.
- 31 Donahue, N. M., Robinson, A. L., Trump, E. R., Riipinen, I. and Kroll, J. H.: Volatility and Aging of
32 Atmospheric Organic Aerosol, in *Atmospheric and Aerosol Chemistry*, vol. 339, edited by V. F. McNeill
33 and P. A. Ariya, pp. 97–143, Springer-Verlag Berlin, Berlin., 2012.
- 34 El Haddad, I., Marchand, N., Wortham, H., Piot, C., Besombes, J.-L., Cozic, J., Chauvel, C., Armengaud,
35 A., Robin, D., and Jaffrezo, J.-L.: Primary sources of PM_{2.5} organic aerosol in an industrial
36 Mediterranean city, Marseille, *Atmos. Chem. Phys.*, 11, 2039–2058, [https://doi.org/10.5194/acp-11-
37 2039-2011](https://doi.org/10.5194/acp-11-2039-2011), 2011.
- 38 Fiore, A. M., Naik, V. and Leibensperger, E. M.: Air Quality and Climate Connections, *J. Air Waste*
39 *Manag. Assoc.*, 65(6), 645–685, doi:10.1080/10962247.2015.1040526, 2015.



- 1 Flores, R. M. and Doskey, P. V.: Evaluation of multistep derivatization methods for identification and
2 quantification of oxygenated species in organic aerosol, *J. Chromatogr. A*, 1418, 1–11,
3 doi:10.1016/j.chroma.2015.09.041, 2015.
- 4 Fridlind, A. M., Jacobson, M. Z., Kerminen, V. M., Hillamo, R. E., Ricard, V., and Jaffrezo, J. L.: Analysis
5 of gas-aerosol partitioning in the Arctic: Comparison of size-resolved equilibrium model results with
6 field data, *J. Geophys. Res.*, 105, 19 891– 19 903, 2000.
- 7 Fruekilde, P., Hjorth, J., Jensen, N. R., Kotzias, D. and Larsen, B.: Ozonolysis at vegetation surfaces : a
8 source of acetone, 4-oxopentanal, 6-methyl-5-hepten-2-one, and geranyl acetone in the
9 troposphere, *Atmos. Environ.*, 32(11), 1893–1902, 1998.
- 10 Fu, P., Kawamura, K., Chen, J. and Barrie, L. A.: Isoprene, monoterpene, and sesquiterpene oxidation
11 products in the high Arctic aerosols during late winter to early summer, *Environ. Sci. Technol.*, 43(11),
12 4022–4028, doi:10.1021/es803669a, 2009.
- 13 Fujiwara, F., Guiñez, M., Cerutti, S. and Smichowski, P.: UHPLC-(+)APCI-MS/MS determination of
14 oxygenated and nitrated polycyclic aromatic hydrocarbons in airborne particulate matter and tree
15 barks collected in Buenos Aires city, *Microchem. J.*, 116, 118–124, doi:10.1016/j.microc.2014.04.004,
16 2014.
- 17 Fuzzi, S., Andreae, M. O., Huebert, B. J., Kulmala, M., Bond, T. C., Boy, M., Doherty, S. J., Guenther, A.,
18 Kanakidou, M., Kawamura, K. and others: Critical assessment of the current state of scientific
19 knowledge, terminology, and research needs concerning the role of organic aerosols in the
20 atmosphere, climate, and global change, *Atmospheric Chem. Phys.*, 6(7), 2017–2038, 2006.
- 21 Gallimore, P. J., Giorio, C., Mahon, B. M., and Kalberer, M.: Online molecular characterisation of
22 organic aerosols in an atmospheric chamber using extractive electrospray ionisation mass
23 spectrometry, *Atmos. Chem. Phys.*, 17, 14485–14500, <https://doi.org/10.5194/acp-17-14485-2017>,
24 2017.
- 25 Gao, S., Keywood, M., Ng, N. L., Surratt, J., Varutbangkul, V., Bahreini, R., Flagan, R. C. and Seinfeld, J.
26 H.: Low-Molecular-Weight and Oligomeric Components in Secondary Organic Aerosol from the
27 Ozonolysis of Cycloalkenes and α -Pinene, *J. Phys. Chem. A*, 108(46), 10147–10164,
28 doi:10.1021/jp047466e, 2004a.
- 29 Gao, S., Ng, N. L., Keywood, M., Varutbangkul, V., Bahreini, R., Nenes, A., He, J., Yoo, K. Y.,
30 Beauchamp, J. L., Hodyss, R. P., Flagan, R. C. and Seinfeld, J. H.: Particle Phase Acidity and Oligomer
31 Formation in Secondary Organic Aerosol, *Environ. Sci. Technol.*, 38(24), 6582–6589,
32 doi:10.1021/es049125k, 2004b.
- 33 Glasius, M. and Goldstein, A. H.: Recent discoveries and future challenges in atmospheric organic
34 chemistry, *Environ. Sci. Technol.*, doi:10.1021/acs.est.5b05105, 2016.
- 35 Goldstein, A. H. and Galbally, I. E.: Known and unexplored organic constituents in the earth's
36 atmosphere, *Environ. Sci. Technol.*, 41(5), 1514–1521, 2007.
- 37 Hallquist, M., Wenger, J. C., Baltensperger, U., Rudich, Y., Simpson, D., Claeys, M., Dommen, J.,
38 Donahue, N. M., George, C., Goldstein, A. H., Hamilton, J. F., Herrmann, H., Hoffmann, T., Iinuma, Y.,
39 Jang, M., Jenkin, M. E., Jimenez, J. L., Kiendler-Scharr, A., Maenhaut, W., McFiggans, G., Mentel, T. F.,
40 Monod, A., Prévôt, A. S. H., Seinfeld, J. H., Surratt, J. D., Szmigielski, R. and Wildt, J.: The formation,
41 properties and impact of secondary organic aerosol: current and emerging issues, *Atmos Chem Phys*,
42 9(14), 5155–5236, doi:10.5194/acp-9-5155-2009, 2009.



- 1 Hamilton, J. F., Webb, P. J., Lewis, A. C., Hopkins, J. R., Smith, S. and Davy, P.: Partially oxidised
2 organic components in urban aerosol using GCXGC-TOF/MS, *Atmospheric Chem. Phys.*, 4(5), 1279–
3 1290, 2004.
- 4 Hansel, A., Jordan, A., Holzinger, R., Prazeller, P., Vogel, W. and Lindinger, W.: Proton transfer
5 reaction mass spectrometry: on-line trace gas analysis at the ppb level, *Int. J. Mass Spectrom. Ion*
6 *Process.*, 149–150, 609–619, doi:10.1016/0168-1176(95)04294-U, 1995.
- 7 Hastings, W. P., Koehler, C. A., Bailey, E. L. and De Haan, D. O.: Secondary Organic Aerosol Formation
8 by Glyoxal Hydration and Oligomer Formation: Humidity Effects and Equilibrium Shifts during
9 Analysis, *Environ. Sci. Technol.*, 39(22), 8728–8735, doi:10.1021/es050446l, 2005.
- 10 Hammes, J., Lutz, A., Mentel, T., Faxon, C., and Hallquist, M.: Carboxylic acids from limonene
11 oxidation by ozone and hydroxyl radicals: insights into mechanisms derived using a FIGAERO-CIMS,
12 *Atmos. Chem. Phys.*, 19, 13037–13052, <https://doi.org/10.5194/acp-19-13037-2019>, 2019.
- 13 Hays, M. D. and Lavrich, R. J.: Developments in direct thermal extraction gas chromatography-mass
14 spectrometry of fine aerosols, *TrAC Trends Anal. Chem.*, 26(2), 88–102,
15 doi:10.1016/j.trac.2006.08.007, 2007.
- 16 Heald, C. L., Kroll, J. H., Jimenez, J. L., Docherty, K. S., DeCarlo, P. F., Aiken, A. C., Chen, Q., Martin, S.
17 T., Farmer, D. K. and Artaxo, P.: A simplified description of the evolution of organic aerosol
18 composition in the atmosphere: Van Krevelen Diagram of organic aerosol, *Geophys. Res. Lett.*, 37(8),
19 n/a–n/a, doi:10.1029/2010GL042737, 2010.
- 20 Healy, R. M., Wenger, J. C., Metzger, A., Duplissy, J., Kalberer, M. and Dommen, J.: Gas/particle
21 partitioning of carbonyls in the photooxidation of isoprene and 1,3,5-trimethylbenzene, *Atmos Chem*
22 *Phys.*, 8(12), 3215–3230, doi:10.5194/acp-8-3215-2008, 2008.
- 23 Ho, S. S. H. and Yu, J. Z.: Feasibility of Collection and Analysis of Airborne Carbonyls by On-Sorbent
24 Derivatization and Thermal Desorption, *Anal. Chem.*, 74(6), 1232–1240, doi:10.1021/ac015708q,
25 2002.
- 26 Ho, S. S. H., Chow, J. C., Watson, J. G., Ip, H. S. S., Ho, K. F., Dai, W. T., and Cao, J.: Biases in ketone
27 measurements using DNPHcoated solid sorbent cartridges, *Anal. Methods-UK*, 6, 967–974,
28 <https://doi.org/10.1039/C3AY41636D>, 2014.
- 29 Holzinger, R., Acton, W. J. F., Bloss, W. J., Breitenlechner, M., Crilley, L. R., Dusanter, S., Gonin, M.,
30 Gros, V., Keutsch, F. N., Kiendler-Scharr, A., Kramer, L. J., Krechmer, J. E., Languille, B., Locoge, N.,
31 Lopez-Hilfiker, F., Materić, D., Moreno, S., Nemitz, E., Quéléver, L. L. J., Sarda Esteve, R., Sauvage, S.,
32 Schallhart, S., Sommariva, R., Tillmann, R., Wedel, S., Worton, D. R., Xu, K., and Zaytsev, A.: Validity
33 and limitations of simple reaction kinetics to calculate concentrations of organic compounds from ion
34 counts in PTR-MS, *Atmos. Meas. Tech.*, 12, 6193–6208, <https://doi.org/10.5194/amt-12-6193-2019>,
35 2019.
- 36 Iinuma, Y., Böge, O., Gnauk, T. and Herrmann, H.: Aerosol-chamber study of the α -pinene/O₃
37 reaction : influence of particle acidity on aerosol yields and products, *Atmos. Environ.*, 38(5), 761–
38 773, doi:10.1016/j.atmosenv.2003.10.015, 2004.
- 39 Jacobson, M. C., Hansson, H.-C., Noone, K. J. and Charlson, R. J.: Organic atmospheric aerosols:
40 Review and state of the science, *Rev. Geophys.*, 38(2), 267–294, doi:10.1029/1998RG000045, 2000.



- 1 Jaffrezo, J. L., Calas, N., and Bouchet, M.: Carboxylic acids measurements with ionic chromatography,
2 *Atmos. Environ.*, 32, 2705–2708, 1998.
- 3 Jang, M. and Kamens, R. M.: Atmospheric secondary aerosol formation by heterogeneous reactions
4 of aldehydes in the presence of a sulfuric acid aerosol catalyst, *Environ. Sci. Technol.*, 35(24), 4758–
5 4766, doi:10.1021/es010790s, 2001.
- 6 Jang, M., Czoschke, N. M., Lee, S. and Kamens, R. M.: Heterogeneous Atmospheric Aerosol
7 Production by Acid-Catalyzed Particle-Phase Reactions, *Science*, 298(5594), 814–817,
8 doi:10.1126/science.1075798, 2002.
- 9 Jang, M., Carroll, B., Chandramouli, B. and Kamens, R. M.: Particle growth by acid-catalyzed
10 heterogeneous reactions of organic carbonyls on preexisting aerosols, *Environ. Sci. Technol.*, 37(17),
11 3828–3837, doi:10.1021/es021005u, 2003.
- 12 Jiang, J., Aksoyoglu, S., El-Haddad, I., Ciarelli, G., Denier van der Gon, H. A. C., Canonaco, F., Gilardoni,
13 S., Paglione, M., Minguillón, M. C., Favez, O., Zhang, Y., Marchand, N., Hao, L., Virtanen, A., Florou, K.,
14 O'Dowd, C., Ovadnevaite, J., Baltensperger, U., and Prévôt, A. S. H.: Sources of organic aerosols in
15 Europe: a modeling study using CAMx with modified volatility basis set scheme, *Atmos. Chem. Phys.*,
16 19, 15247–15270, <https://doi.org/10.5194/acp-19-15247-2019>, 2019.
- 17 Jimenez, J. L., Jayne, J. T., Shi, Q., Kolb, C. E., Worsnop, D. R., Yourshaw, I., Seinfeld, J. H., Flagan, R. C.,
18 Zhang, X., Smith, K. A., Morris, J. W. and Davidovits, P.: Ambient aerosol sampling using the Aerodyne
19 Aerosol Mass Spectrometer, *J. Geophys. Res. Atmospheres*, 108(D7), 8425,
20 doi:10.1029/2001JD001213, 2003.
- 21 Jimenez, J. L., Canagaratna, M. R., Donahue, N. M., Prevot, A. S. H., Zhang, Q., Kroll, J. H., DeCarlo, P.
22 F., Allan, J. D., Coe, H., Ng, N. L., Aiken, A. C., Docherty, K. S., Ulbrich, I. M., Grieshop, A. P., Robinson,
23 A. L., Duplissy, J., Smith, J. D., Wilson, K. R., Lanz, V. A., Hueglin, C., Sun, Y. L., Tian, J., Laaksonen, A.,
24 Raatikainen, T., Rautiainen, J., Vaattovaara, P., Ehn, M., Kulmala, M., Tomlinson, J. M., Collins, D. R.,
25 Cubison, M. J., E., Dunlea, J., Huffman, J. A., Onasch, T. B., Alfarra, M. R., Williams, P. I., Bower, K.,
26 Kondo, Y., Schneider, J., Drewnick, F., Borrmann, S., Weimer, S., Demerjian, K., Salcedo, D., Cottrell,
27 L., Griffin, R., Takami, A., Miyoshi, T., Hatakeyama, S., Shimono, A., Sun, J. Y., Zhang, Y. M., Dzepina,
28 K., Kimmel, J. R., Sueper, D., Jayne, J. T., Herndon, S. C., Trimborn, A. M., Williams, L. R., Wood, E. C.,
29 Middlebrook, A. M., Kolb, C. E., Baltensperger, U. and Worsnop, D. R.: Evolution of Organic Aerosols
30 in the Atmosphere, *Science*, 326(5959), 1525–1529, doi:10.1126/science.1180353, 2009.
- 31 Kajos, M. K., Rantala, P., Hill, M., Hellen, H., Aalto, J., Patokoski, J., Taipale, R., Hoerger, C. C.,
32 Reimann, S., Ruuskanen, T. M., Rinne, J. and Petaja, T.: Ambient measurements of aromatic and
33 oxidized VOCs by PTR-MS and GC-MS: intercomparison between four instruments in a boreal forest
34 in Finland, *Atmospheric Meas. Tech.*, 8(10), 4453–4473, doi:10.5194/amt-8-4453-2015, 2015.
- 35 Kalberer, M., Paulsen, D., Sax, M., Steinbacher, M., Dommen, J., Prevot, A. S. H., Fisseha, R.,
36 Weingartner, E., Frankevich, V., Zenobi, R. and Baltensperger, U.: Identification of Polymers as Major
37 Components of Atmospheric Organic Aerosols, *Science*, 303(5664), 1659–1662,
38 doi:10.1126/science.1092185, 2004.
- 39 Kanakidou, M., Seinfeld, J. H., Pandis, S. N., Barnes, I., Dentener, F. J., Facchini, M. C., Van Dingenen,
40 R., Ervens, B., Nenes, A., Nielsen, C. J., Swietlicki, E., Putaud, J. P., Balkanski, Y., Fuzzi, S., Horth, J.,
41 Moortgat, G. K., Winterhalter, R., Myhre, C. E. L., Tsigaridis, K., Vignati, E., Stephanou, E. G. and
42 Wilson, J.: Organic aerosol and global climate modelling: a review, *Atmos Chem Phys*, 5(4), 1053–
43 1123, doi:10.5194/acp-5-1053-2005, 2005.



- 1 Kitanovski, Z., Grgić, I. and Veber, M.: Characterization of carboxylic acids in atmospheric aerosols
2 using hydrophilic interaction liquid chromatography tandem mass spectrometry, *J. Chromatogr. A*,
3 1218(28), 4417–4425, doi:10.1016/j.chroma.2011.05.020, 2011.
- 4 Kulmala, M., Kontkanen, J., Junninen, H., Lehtipalo, K., Manninen, H. E., Nieminen, T., Petäjä, T., Sipilä
5 M., M., Schobesberger, S., Rantala, P., Franchin, A., Jokinen, T., Järvinen, E., Äijälä, M., Kangasluoma,
6 J., Hakala, J., Aalto, P. P., Paasonen, P., Mikkilä, J., Vanhanen, J., Aalto, J., Hakola, H., Makkonen, U.,
7 Ruuskanen, T., Mauldin, R. L., Duplissy, J., Vehkamäki, H., Bäck, J., Kortelainen, A., Riipinen, I., Kurtén,
8 T., Johnston, M. V., Smith, J. N., Ehn, M., Mentel, T. F., Lehtinen, K. E. J., Laaksonen, A., Kerminen, V.-
9 M., and Worsnop, D. R.: Direct Observations of Atmospheric Aerosol Nucleation, *Science*, 339, 943–
10 946, <https://doi.org/10.1126/science.1227385>, 2013.
- 11 Lelieveld, J.: Global Air Pollution Crossroads over the Mediterranean, *Science*, 298(5594), 794–799,
12 doi:10.1126/science.1075457, 2002.
- 13 Li, Y., Pöschl, U., and Shiraiwa, M.: Molecular corridors and parameterizations of volatility in the
14 chemical evolution of organic aerosols, *Atmos. Chem. Phys.*, 16, 3327–3344,
15 <https://doi.org/10.5194/acp-16-3327-2016>, 2016.
- 16 Liang, C., Pankow, J. F., Odum, J. R. and Seinfeld, J. H.: Gas/Particle Partitioning of Semivolatile
17 Organic Compounds To Model Inorganic, Organic, and Ambient Smog Aerosols, *Environ. Sci.*
18 *Technol.*, 31(11), 3086–3092, doi:10.1021/es9702529, 1997.
- 19 Liggio, J., Li, S.-M. and McLaren, R.: Heterogeneous reactions of glyoxal on particulate matter :
20 identification of acetals and sulfate esters, *Environ. Sci. Technol.*, 39(6), 1532–1541,
21 doi:10.1021/es048375y, 2005a.
- 22 Liggio, J., Li, S.-M. and McLaren, R.: Reactive uptake of glyoxal by particulate matter, *J. Geophys. Res.*
23 *Atmospheres*, 110(D10), D10304, doi:10.1029/2004JD005113, 2005b.
- 24 Lim, Y. B., Tan, Y., Perri, M. J., Seitzinger, S. P. and Turpin, B. J.: Aqueous chemistry and its role in
25 secondary organic aerosol (SOA) formation, *Atmospheric Chem. Phys.*, 10(21), 10521–10539,
26 doi:10.5194/acp-10-10521-2010, 2010.
- 27 Liu, F., Duan, F.-K., Li, H.-R., Ma, Y.-L., He, K.-B. and Zhang, Q.: Solid Phase Microextraction/Gas
28 Chromatography-Tandem Mass Spectrometry for Determination of Polycyclic Aromatic
29 Hydrocarbons in Fine Aerosol in Beijing, *Chin. J. Anal. Chem.*, 43(4), 540–546, doi:10.1016/S1872-
30 2040(15)60818-0, 2015.
- 31 Matsunaga, S.: Variation on the atmospheric concentrations of biogenic carbonyl compounds and
32 their removal processes in the northern forest at Moshiri, Hokkaido Island in Japan, *J. Geophys. Res.*,
33 109(D4), doi:10.1029/2003JD004100, 2004.
- 34 Michoud, V., Sciare, J., Sauvage, S., Dusanter, S., Léonardis, T., Gros, V., Kalogridis, C., Zannoni, N.,
35 Féron, A., Petit, J.-E., Crenn, V., Baisnée, D., Sarda-Estève, R., Bonnaire, N., Marchand, N., DeWitt, H.
36 L., Pey, J., Colomb, A., Gheusi, F., Szidat, S., Stavroulas, I., Borbon, A., and Locoge, N.: Organic carbon
37 at a remote site of the western Mediterranean Basin: sources and chemistry during the ChArMEx
38 SOP2 field experiment, *Atmos. Chem. Phys.*, 17, 8837–8865, [https://doi.org/10.5194/acp-17-8837-](https://doi.org/10.5194/acp-17-8837-2017)
39 2017, 2017.
- 40 Michoud, V., Sauvage, S., Léonardis, T., Fronval, I., Kukui, A., Locoge, N., and Dusanter, S.: Field
41 measurements of methylglyoxal using proton transfer reaction time-of-flight mass spectrometry and



- 1 comparison to the DNPH–HPLC–UV method, *Atmos. Meas. Tech.*, **11**, 5729–5740,
2 <https://doi.org/10.5194/amt-11-5729-2018>, 2018.
- 3 Millán, M. M., Salvador, R., Mantilla, E. and Kallos, G.: Photooxidant dynamics in the Mediterranean
4 basin in summer: Results from European research projects, *J. Geophys. Res. Atmospheres*, **102**(D7),
5 8811–8823, doi:10.1029/96JD03610, 1997.
- 6 Minguillón, M. C., Ripoll, A., Pérez, N., Prévôt, A. S. H., Canonaco, F., Querol, X. and Alastuey, A.:
7 Chemical characterization of submicron regional background aerosols in the western Mediterranean
8 using an Aerosol Chemical Speciation Monitor, *Atmospheric Chem. Phys.*, **15**(11), 6379–6391,
9 doi:10.5194/acp-15-6379-2015, 2015.
- 10 Moller, B., Rarey, J. and Ramjugernath, D.: Estimation of the vapour pressure of non-electrolyte
11 organic compounds via group contributions and group interactions, *J. Mol. Liq.*, **143**(1), 52–63,
12 doi:10.1016/j.molliq.2008.04.020, 2008.
- 13 Moroni, B., Castellini, S., Crocchianti, S., Piazzalunga, A., Fermo, P., Scardazza, F. and Cappelletti, D.:
14 Ground-based measurements of long-range transported aerosol at the rural regional background site
15 of Monte Martano (Central Italy), *Atmospheric Res.*, **155**, 26–36,
16 doi:10.1016/j.atmosres.2014.11.021, 2015.
- 17 Myrdal, P. B. and Yalkowsky, S. H.: Estimating Pure Component Vapor Pressures of Complex Organic
18 Molecules, *Ind. Eng. Chem. Res.*, **36**(6), 2494–2499, doi:10.1021/ie950242l, 1997.
- 19 Nannoolal, Y., Rarey, J., Ramjugernath, D. and Cordes, W.: Estimation of pure component properties:
20 Part 1. Estimation of the normal boiling point of non-electrolyte organic compounds via group
21 contributions and group interactions, *Fluid Phase Equilibria*, **226**, 45–63,
22 doi:10.1016/j.fluid.2004.09.001, 2004.
- 23 Nannoolal, Y., Rarey, J. and Ramjugernath, D.: Estimation of pure component properties: Part 3.
24 Estimation of the vapor pressure of non-electrolyte organic compounds via group contributions and
25 group interactions, *Fluid Phase Equilibria*, **269**(1–2), 117–133, doi:10.1016/j.fluid.2008.04.020, 2008.
- 26 Ng, N. L., Canagaratna, M. R., Zhang, Q., Jimenez, J. L., Tian, J., Ulbrich, I. M., Kroll, J. H., Docherty, K.
27 S., Chhabra, P. S., Bahreini, R., Murphy, S. M., Seinfeld, J. H., Hildebrandt, L., Donahue, N. M.,
28 DeCarlo, P. F., Lanz, V. A., Prévôt, A. S. H., Dinar, E., Rudich, Y. and Worsnop, D. R.: Organic aerosol
29 components observed in Northern Hemispheric datasets from Aerosol Mass Spectrometry, *Atmos
30 Chem Phys*, **10**(10), 4625–4641, doi:10.5194/acp-10-4625-2010, 2010.
- 31 Ng, N. L., Canagaratna, M. R., Jimenez, J. L., Chhabra, P. S., Seinfeld, J. H. and Worsnop, D. R.:
32 Changes in organic aerosol composition with aging inferred from aerosol mass spectra, *Atmospheric
33 Chem. Phys.*, **11**(13), 6465–6474, doi:10.5194/acp-11-6465-2011, 2011.
- 34 Nguyen, T. B., Laskin, J., Laskin, A. and Nizkorodov, S. A.: Nitrogen-Containing Organic Compounds
35 and Oligomers in Secondary Organic Aerosol Formed by Photooxidation of Isoprene, *Environ. Sci.
36 Technol.*, **45**(16), 6908–6918, doi:10.1021/es201611n, 2011.
- 37 Nguyen, T. B., Nizkorodov, S. A., Laskin, A. and Laskin, J.: An approach toward quantification of
38 organic compounds in complex environmental samples using high-resolution electrospray ionization
39 mass spectrometry, *Anal. Methods*, **5**(1), 72, doi:10.1039/c2ay25682g, 2013.
- 40 Nicolas, J. B.: Caractérisation physico-chimique de l'aérosol troposphérique en Méditerranée :
41 sources et devenir, Université de Versailles Saint-Quentin-en-Yvelines (UVSQ). [online] Available



- 1 from: <http://www.uvsq.fr/caracterisation-physico-chimique-de-l-aerosol-tropospherique-en-mediterranee-sources-et-devenir-par-jose-nicolas-303880.kjsp> (Accessed 2 February 2016), 2013.
- 3 Nozière, B., Kalberer, M., Claeys, M., Allan, J., D'Anna, B., Decesari, S., Finessi, E., Glasius, M., Grgić, I.,
4 Hamilton, J. F., Hoffmann, T., Iinuma, Y., Jaoui, M., Kahnt, A., Kampf, C. J., Kourtchev, I., Maenhaut,
5 W., Marsden, N., Saarikoski, S., Schnelle-Kreis, J., Surratt, J. D., Szidat, S., Szmigielski, R. and
6 Wisthaler, A.: The molecular identification of organic compounds in the atmosphere : state of the art
7 and challenges, *Chem. Rev.*, 150203102816008, doi:10.1021/cr5003485, 2015.
- 8 Orsini, D. A., Ma, Y., Sullivan, A., Sierau, B., Baumann, K. and Weber, R. J.: Refinements to the
9 particle-into-liquid sampler (PILS) for ground and airborne measurements of water soluble aerosol
10 composition, *Atmos. Environ.*, 37(9–10), 1243–1259, doi:10.1016/S1352-2310(02)01015-4, 2003.
- 11 Pankow, J. F.: An absorption model of gas/particle partitioning of organic compounds in the
12 atmosphere, *Atmos. Environ.*, 28(2), 185–188, 1994.
- 13 Parshintsev, J. and Hyötyläinen, T.: Methods for characterization of organic compounds in
14 atmospheric aerosol particles, *Anal. Bioanal. Chem.*, 407(20), 5877–5897, doi:10.1007/s00216-014-
15 8394-3, 2015.
- 16 Parshintsev, J., Rasanen, R., Hartonen, K., Kulmala, M. and Riekkola, M.-L.: Analysis of organic
17 compounds in ambient aerosols collected with the particle-into-liquid sampler, *Boreal Environ. Res.*,
18 14(4), 630–640, 2009.
- 19 Pietrogrande, M. C., Bacco, D. and Mercuriali, M.: GC–MS analysis of low-molecular-weight
20 dicarboxylic acids in atmospheric aerosol: comparison between silylation and esterification
21 derivatization procedures, *Anal. Bioanal. Chem.*, 396(2), 877–885, doi:10.1007/s00216-009-3212-z,
22 2009.
- 23 Pöschl, U.: Atmospheric Aerosols : composition, transformation, climate and health effects, *Angew.
24 Chem. Int. Ed.*, 44(46), 7520–7540, doi:10.1002/anie.200501122, 2005.
- 25 Querol, X., Pey, J., Pandolfi, M., Alastuey, A., Cusack, M., Pérez, N., Moreno, T., Viana, M.,
26 Mihalopoulos, N., Kallos, G. and Kleanthous, S.: African dust contributions to mean ambient PM10
27 mass-levels across the Mediterranean Basin, *Atmos. Environ.*, 43(28), 4266–4277,
28 doi:10.1016/j.atmosenv.2009.06.013, 2009a.
- 29 Querol, X., Alastuey, A., Pey, J., Cusack, M., Pérez, N., Mihalopoulos, N., Theodosi, C., Gerasopoulos,
30 E., Kubilay, N. and Koçak, M.: Variability in regional background aerosols within the Mediterranean,
31 *Atmos Chem Phys*, 9(14), 4575–4591, doi:10.5194/acp-9-4575-2009, 2009b.
- 32 Raventos-Duran, T., Camredon, M., Valorso, R., Mouchel-Vallon, C. and Aumont, B.: Structure-activity
33 relationships to estimate the effective Henry's law constants of organics of atmospheric interest,
34 *Atmos Chem Phys*, 10(16), 7643–7654, doi:10.5194/acp-10-7643-2010, 2010.
- 35 Ripoll, A., Minguillón, M. C., Pey, J., Pérez, N., Querol, X. and Alastuey, A.: Joint analysis of continental
36 and regional background environments in the western Mediterranean: PM1 and PM10
37 concentrations and composition, *Atmospheric Chem. Phys.*, 15(2), 1129–1145, doi:10.5194/acp-15-
38 1129-2015, 2015.
- 39 Robinson, A. L., Donahue, N. M., Shrivastava, M. K., Weitkamp, E. A., Sage, A. M., Grieshop, A. P.,
40 Lane, T. E., Pierce, J. R. and Pandis, S. N.: Rethinking organic aerosols : semivolatile emissions and
41 photochemical aging, *Science*, 315(5816), 1259–1262, doi:10.1126/science.1133061, 2007.



- 1 Rossignol, S.: Développement d'une méthode de prélèvement simultané et d'analyse chimique des
2 phases gazeuse et particulaire atmosphériques pour une approche multiphasique de l'aérosol
3 organique secondaire, Paris 7. [online] Available from: <http://www.theses.fr/2012PA077208>
4 (Accessed 14 February 2016), 2012.
- 5 Rossignol, S., Chiappini, L., Perraudin, E., Rio, C., Fable, S., Valorso, R. and Doussin, J. F.: Development
6 of a parallel sampling and analysis method for the elucidation of gas/particle partitioning of
7 oxygenated semi-volatile organics: a limonene ozonolysis study, *Atmospheric Meas. Tech.*, 5(6),
8 1459–1489, doi:10.5194/amt-5-1459-2012, 2012.
- 9 Rossignol, S., Couvidat, F., Rio, C., Fable, S., Grignon, G., Savelli, Pailly, O., Leoz-Garziandia, E.,
10 Doussin, J.-F. and Chiappini, L.: Organic aerosol molecular composition and gas–particle partitioning
11 coefficients at a Mediterranean site (Corsica), *J. Environ. Sci.*, 40, 92–104,
12 doi:10.1016/j.jes.2015.11.017, 2016.
- 13 Samake A, Jaffrezo JL, Favez O, Weber S, Jacob V, Albinet A, Riffault V, Perdrix E, Waked A, Golly B,
14 Salameh D, Chevrier F, Oliveira D, Bonnaire N, Besombes JL, Martins JMF, Conil S, Guillaud G, Mesbah
15 B, Rocq B, Robic PY, Hulin A, Le Meur S, Descheemaeker M, Chretien E, Marchand N, and Uzu G.
16 (2019) Polyols and Glucose Particulate Species as Tracers of Primary Biogenic Organic Aerosols at 28
17 French Sites. *Atmos. Chem. Phys.*, doi.org/10.5194/acp-19-3357-2019.
- 18 Schoene, K., Bruckert, H.-J., Steinhanses, J. and König, A.: Two stage derivatization with N-(tert.-
19 butyldimethylsilyl)-N-methyl-trifluoroacetamide (MTBSTFA) and N-methyl-bis-
20 (trifluoroacetamide)(MBTFA) for the gas-chromatographic analysis of OH-, SH-and NH-compounds,
21 *Fresenius J. Anal. Chem.*, 348(5-6), 364–370, 1994.
- 22 Sciare, J., d'Argouges, O., Sarda-Estève, R., Gaimoz, C., Dolgorouky, C., Bonnaire, N., Favez, O.,
23 Bonsang, B. and Gros, V.: Large contribution of water-insoluble secondary organic aerosols in the
24 region of Paris (France) during wintertime, *J. Geophys. Res. Atmospheres*, 116(D22), D22203,
25 doi:10.1029/2011JD015756, 2011.
- 26 Seinfeld, J. H. and Pankow, J. F.: Organic atmospheric particulate material, *Annu. Rev. Phys. Chem.*,
27 54(1), 121–140, doi:10.1146/annurev.physchem.54.011002.103756, 2003.
- 28 Shiraiwa, M., Ammann, M., Koop, T. and Pöschl, U.: Gas uptake and chemical aging of semisolid
29 organic aerosol particles, *Proc. Natl. Acad. Sci.*, 108(27), 11003–11008, 2011.
- 30 Shrivastava, M. K., Subramanian, R., Rogge, W. F. and Robinson, A. L.: Sources of organic aerosol :
31 positive matrix factorization of molecular marker data and comparison of results from different
32 source apportionment models, *Atmos. Environ.*, 41(40), 9353–9369,
33 doi:10.1016/j.atmosenv.2007.09.016, 2007.
- 34 Soonsin, V., Zardini, A. A., Marcolli, C., Zuend, A. and Krieger, U. K.: The vapor pressures and activities
35 of dicarboxylic acids reconsidered: the impact of the physical state of the aerosol, *Atmos Chem Phys*,
36 10(23), 11753–11767, doi:10.5194/acp-10-11753-2010, 2010.
- 37 Sorooshian, A., Brechtel, F. J., Ma, Y. L., Weber, R. J., Corless, A., Flagan, R. C., and Seinfeld, J. H.:
38 Modeling and characterization of a particle-into-liquid sampler (PILS), *Aerosol Sci. Tech.*, 40, 396–
39 409, 2006.
- 40 Srivastava, D., Tomaz, S., Favez, O., Lanzafame, G. M., Golly, B., Besombes, J.-L., Alleman, L. Y.,
41 Jaffrezo, J.-L., Jacob, V., Perraudin, E., Villenave, E., and Albinet, A.: Speciation of organic fraction



- 1 does matter for source apportionment. Part 1: A one-year campaign in Grenoble (France), *Sci. Total*
2 *Environ.*, 624, 1598–1611, 2018
- 3 Tolocka, M. P., Jang, M., Ginter, J. M., Cox, F. J., Kamens, R. M. and Johnston, M. V.: Formation of
4 oligomers in secondary organic aerosol, *Environ. Sci. Technol.*, 38(5), 1428–1434,
5 doi:10.1021/es035030r, 2004.
- 6 Valach, A. C., Langford, B., Nemitz, E., MacKenzie, A. R. and Hewitt, C. N.: Concentrations of selected
7 volatile organic compounds at kerbside and background sites in central London, *Atmos. Environ.*, 95,
8 456–467, doi:10.1016/j.atmosenv.2014.06.052, 2014.
- 9 van Drooge, B. L., Nikolova, I. and Ballesta, P. P.: Thermal desorption gas chromatography–mass
10 spectrometry as an enhanced method for the quantification of polycyclic aromatic hydrocarbons
11 from ambient air particulate matter, *J. Chromatogr. A*, 1216(18), 4030–4039,
12 doi:10.1016/j.chroma.2009.02.043, 2009.
- 13 Virtanen, A., Joutsensaari, J., Koop, T., Kannosto, J., Yli-Pirilä, P., Leskinen, J., Mäkelä, J. M.,
14 Holopainen, J. K., Pöschl, U., Kulmala, M., Worsnop, D. R. and Laaksonen, A.: An amorphous solid
15 state of biogenic secondary organic aerosol particles, *Nature*, 467(7317), 824–827,
16 doi:10.1038/nature09455, 2010.
- 17 Washenfelder, R. A., Young, C. J., Brown, S. S., Angevine, W. M., Atlas, E. L., Blake, D. R., Bon, D. M.,
18 Cubison, M. J., de Gouw, J. A., Dusanter, S., Flynn, J., Gilman, J. B., Graus, M., Griffith, S., Grossberg,
19 N., Hayes, P. L., Jimenez, J. L., Kuster, W. C., Lefer, B. L., Pollack, I. B., Ryerson, T. B., Stark, H., Stevens,
20 P. S., and Trainer, M. K.: The glyoxal budget and its contribution to organic aerosol for Los Angeles,
21 California, during CalNex 2010, *J. Geophys. Res.*, 116, D00V02,
22 <https://doi.org/10.1029/2011JD016314>, 2011
- 23 Williams, B. J., Goldstein, A. H., Kreisberg, N. M. and Hering, S. V.: An In-Situ Instrument for Speciated
24 Organic Composition of Atmospheric Aerosols: Thermal Desorption Aerosol GC/MS-FID (TAG),
25 *Aerosol Sci. Technol.*, 40(8), 627–638, doi:10.1080/02786820600754631, 2006.
- 26 Woody, M. C., Baker, K. R., Hayes, P. L., Jimenez, J. L., Koo, B., and Pye, H. O. T.: Understanding
27 sources of organic aerosol during CalNex-2010 using the CMAQ-VBS, *Atmos. Chem. Phys.*, 16, 4081–
28 4100, <https://doi.org/10.5194/acp-16-4081-2016>, 2016.
- 29 Zannoni, N., Gros, V., Sarda Esteve, R., Kalogridis, C., Michoud, V., Dusanter, S., Sauvage, S., Locoge,
30 N., Colomb, A., and Bonsang, B.: Summertime OH reactivity from a receptor coastal site in the
31 Mediterranean Basin, *Atmos. Chem. Phys.*, 17, 12645–12658, [https://doi.org/10.5194/acp-17-12645-](https://doi.org/10.5194/acp-17-12645-2017)
32 2017, 2017.
- 33 Zhang, H., Surratt, J. D., Lin, Y. H., Bapat, J. and Kamens, R. M.: Effect of relative humidity on SOA
34 formation from isoprene/NO photooxidation : enhancement of 2-methylglyceric acid and its
35 corresponding oligoesters under dry conditions, *Atmospheric Chem. Phys.*, 11(13), 6411–6424,
36 doi:10.5194/acp-11-6411-2011, 2011a.
- 37 Zhang, Q., Jimenez, J. L., Canagaratna, M. R., Ulbrich, I. M., Ng, N. L., Worsnop, D. R. and Sun, Y.:
38 Understanding atmospheric organic aerosols via factor analysis of aerosol mass spectrometry: a
39 review, *Anal. Bioanal. Chem.*, 401(10), 3045–3067, doi:10.1007/s00216-011-5355-y, 2011b.
- 40 Zhang, X., Dalleska, N. F., Huang, D. D., Bates, K. H., Sorooshian, A., Flagan, R. C. and Seinfeld, J. H.:
41 Time-resolved molecular characterization of organic aerosols by PILS + UPLC/ESI-Q-TOFMS, *Atmos.*
42 *Environ.*, 130, 180–189, doi:10.1016/j.atmosenv.2015.08.049, 2016.



- 1 Zobrist, B., Soonsin, V., Luo, B. P., Krieger, U. K., Marcolli, C., Peter, T. and Koop, T.: Ultra-slow water
- 2 diffusion in aqueous sucrose glasses, *Phys. Chem. Chem. Phys.*, 13(8), 3514–3526,
- 3 doi:10.1039/C0CP01273D, 2011.
- 4



1 Table 1: Thermal desorption method and GC/MS parameters

Thermal desorption parameters for samples	temperature	300°C
	time	15 minutes
	flow	50 mL min ⁻¹
	split flow	No split flow
Thermal desorption parameters for the trap	Temperature	From -10°C to 300°C
	Time	12 minutes
	flow	10 mL min ⁻¹
Temperature of transfer lines		200°C
GC Parameters	Carrier gas	He
	Carrier gas flow	1 mL min ⁻¹
	Temperature gradient	40°C / 10°C min ⁻¹ / 305°C (10 min)
	Split flow	0.2 mL min ⁻¹
	Transfer line temperature to MS	305 °C
MS parameters	Scan m/z	40 to 800
	Solvent delay	5 min
	Quadrupole temperature	150°C
	EI	
	-Source temperature	230°C
	-Ionization Energy	70 eV
	CI	
-Source temperature	250°C	
-Reagent gas	CH ₄	
-Ionization Energy	50 eV	

2

3



1 Table 2 : List of substitutes used for internal calibration

Substitutes used for carbonyl compounds	Substitutes used for hydroxyl compounds
3-methylbutanal-d2	Pentanoic acid-d9
Butanal-d8	Heptanoic acid-d13
4-methyl-2-pentanone-d5	Succinic acid-d4
Benzaldehyde-d6	2-methyl-d3-2-propyl-1,3-propanediol
Acetophenone-d8	Glycerol-d8
2-hexanone-d5	Tartaric acid-2,3-d2
2,3-butanedione-d5	
2,5-hexanedione-d10	

2

3



- 1 Table 3: meteorological conditions, environmental parameters and mass concentrations of PM₁₀, PM₁
- 2 and organic fraction in PM₁ during the ChArMEx campaign at ERSA

Meteorological and Environmental Parameters	Mean	Median	Max	Min
Temperature (°C)	23	23	32	19
Relative Humidity (%)	70	73	100	27
Wind Speed (m s ⁻¹)	3.6	3.1	13.2	-
O ₃ (ppbv)	65	65	111	42
NO _x (ppbv)	0.57	0.45	4.93	0.06
Mass concentrations (µg m⁻³)	Mean (±1σ)	Median	Max	Min
PM ₁₀	12 (±4.8)	12	31	2
PM ₁	8.4 (±4.4)	8.4	22	0.2
Organic fraction (PM ₁)	3.7 (±1.7)	3.5	8.1	0.2

3



- 1 Table 4: Experimental (averaged over the campaign with $\pm XX\%$ representing 1σ standard deviation
 2 over the campaign) and theoretical partitioning coefficients determined for this study and compared
 3 to previous field and chamber campaigns.

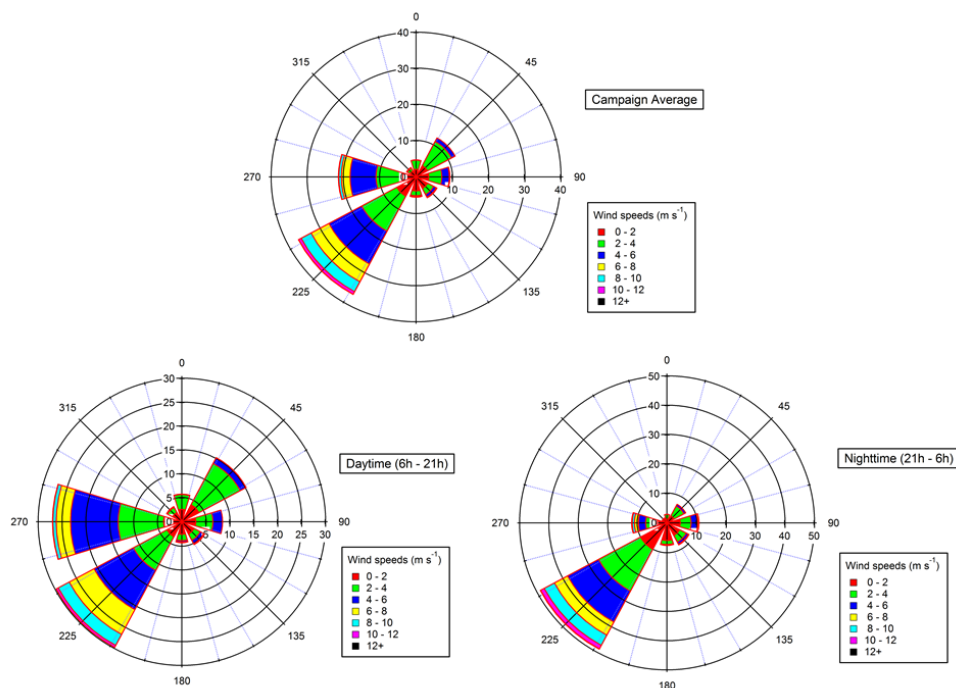
	This study	Corsica ^a	EuPhoRe ^a	Kpt,i MOL ^b	Kpt,i NAN ^c	Kpt,i MYR ^d
Propanal	$6.1 \times 10^{-3} \pm 75\%$	$2.2 \times 10^{-3} \pm 50\%$		2.6×10^{-10}	2.6×10^{-10}	4.7×10^{-10}
Pentanal	$6.5 \times 10^{-4} \pm 106\%^{**}$	$1.8 \times 10^{-4} \pm 51\%$		3.2×10^{-9}	3.2×10^{-9}	3.8×10^{-9}
Hexanal	$1.3 \times 10^{-3} \pm 61\%$			1.0×10^{-8}	1.0×10^{-8}	1.1×10^{-8}
Heptanal	$5.1 \times 10^{-4} \pm 91\%$			3.3×10^{-8}	3.2×10^{-8}	3.4×10^{-8}
Acrolein	$7.3 \times 10^{-4} \pm 74\%$	$6.1 \times 10^{-3} \pm 50\%$		3.6×10^{-10}	3.6×10^{-10}	3.7×10^{-7}
Methacrolein	$7.3 \times 10^{-4} \pm 69\%$			7.2×10^{-10}	7.2×10^{-10}	9.0×10^{-10}
Methyl Vinyl ketone	$5.8 \times 10^{-4} \pm 57\%$			1.3×10^{-9}	1.3×10^{-9}	5.6×10^{-10}
Nopinone	$5.5 \times 10^{-4} \pm 53\%$			1.7×10^{-7}	1.7×10^{-7}	1.9×10^{-7}
Dimethylglyoxal	$5.0 \times 10^{-3} \pm 65\%$	$5.6 \times 10^{-4} \pm 70\%$	$6.2 \times 10^{-4} \pm 47\%$		3.4×10^{-9} *	7.0×10^{-9} *
Methylglyoxal	$3.6 \times 10^{-3} \pm 60\%$	$2.2 \times 10^{-2} \pm 132\%^{**}$	$1.3 \times 10^{-3} \pm 84\%$		8.6×10^{-10} *	2.1×10^{-9} *
Levulinic acid	$5.1 \times 10^{-3} \pm 77\%$			1.7×10^{-5}	4.4×10^{-6}	2.9×10^{-6}
Methacrylic acid	$1.5 \times 10^{-4} \pm 198\%^{**}$			8.4×10^{-8}	7.6×10^{-8}	8.9×10^{-8}
Glycolic acid	$3.1 \times 10^{-2} \pm 268\%^{**}$			8.5×10^{-5}	1.3×10^{-5}	2.0×10^{-6}
Glycerol	$1.1 \times 10^{-2} \pm 62\%$			7.1×10^{-4}	8.4×10^{-4}	1.3×10^{-5}

- 4 ^a Rossignol et al., 2016; ^b Moller et al., 2008 (coupled with Nannoolal et al. (2004) method for boiling point determination); ^c Nannoolal et
 5 al., 2008 (coupled with Nannoolal et al. (2004) method for boiling point determination); ^d Myrdal and Yalkowsky, 1997 (coupled with
 6 Nannoolal et al. (2004) method for boiling point determination)

7 * Coefficients extracted from Rossignol, 2012 at temperature of 300 K other parameter (MW_{om} et ζ) kept similar.

8 ** Partitioning coefficients are comprised between 0 and 1. Experimental uncertainties greater than 100% mean that the experimental
 9 value is comprised between 0 and more than twice its values.

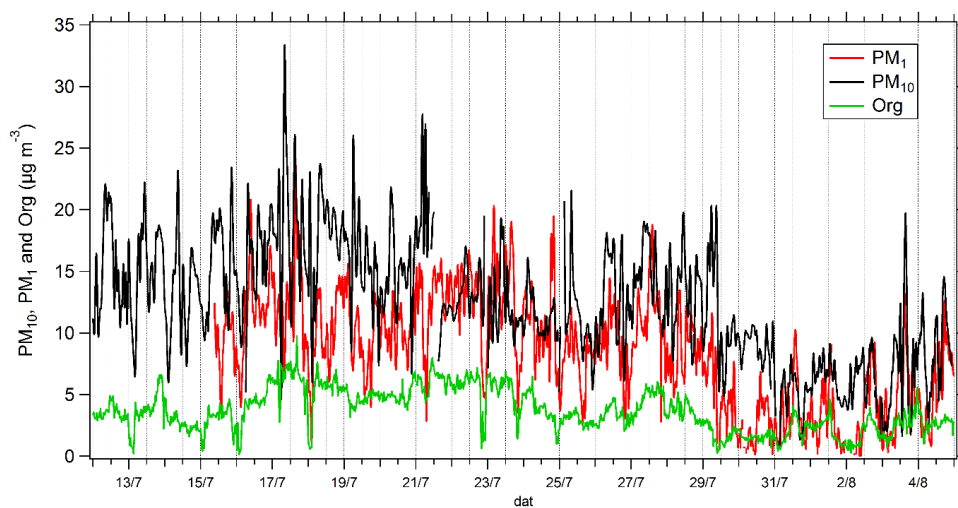
10



1

2 Figure 1 : Wind roses from July 15th to August 5th 2013 (top panel), during daytime only (bottom left
3 panel) and during nighttime only (bottom right panel). Wind direction is expressed in ° and radial axe
4 express the relative occurrence of wind in each 30° sector (%).

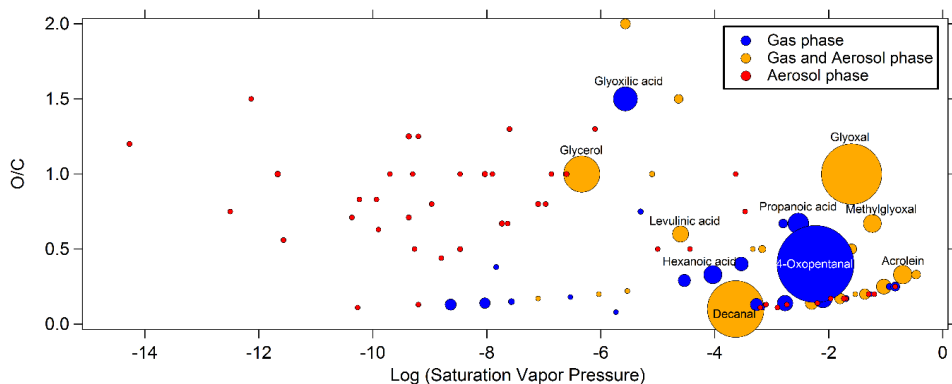
5



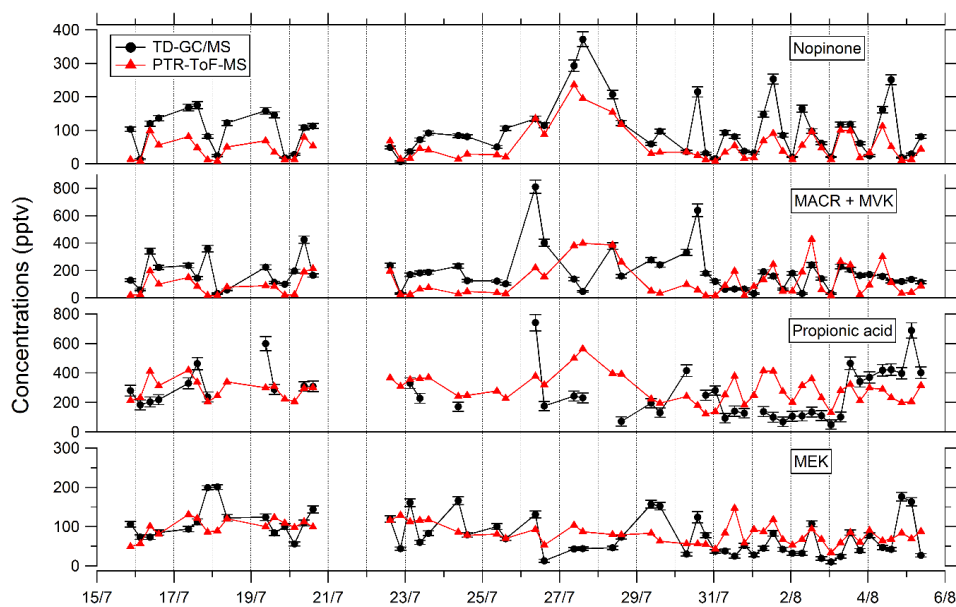
1

2 Figure 2 : Time series of mass concentrations of PM₁₀ (black line), PM₁ (red line) and organic
3 fraction in NR-PM₁ (green line).

4



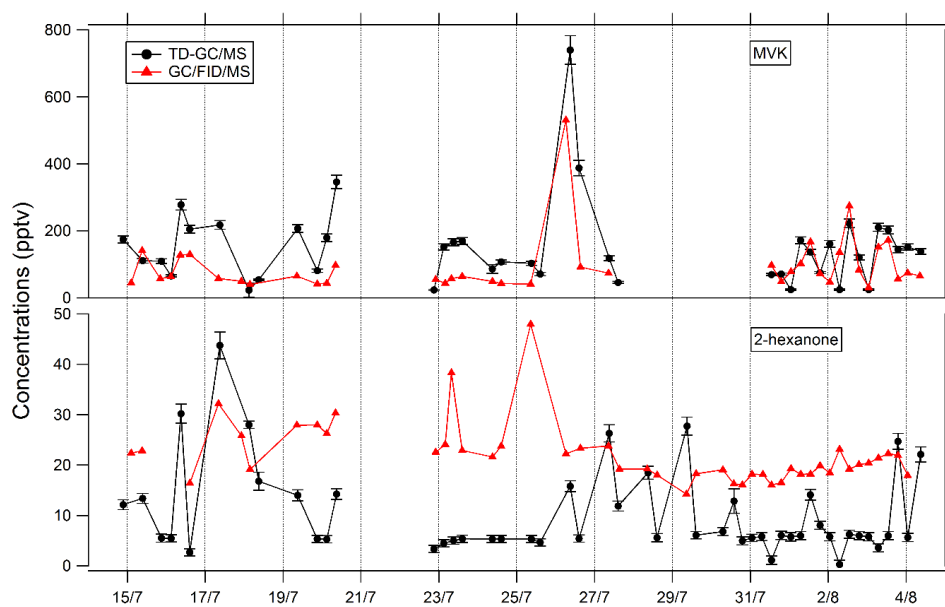
1
2 Figure 3: Distribution of compounds identified by TD-GC/MS during the ChArMEx campaign according
3 to the logarithm of their saturation vapor pressure (horizontal axis) and of their O/C ratio (vertical axis).
4 The phase in which they are detected is color-coded: blue for compounds only detected in the gas
5 phase, red for aerosol phase only and orange for compounds detected in both phases. Each dot
6 represents a single compound and the dot area is proportional to the sum of concentrations if detected
7 in both phases from 0.3 ng m^{-3} for the smallest dot to $3.9 \text{ } \mu\text{g m}^{-3}$ for the biggest one. Name of some
8 noticeable compounds are also given.



1

2 Figure 4 : Comparison of TD-GC/MS data with PTR-ToF-MS data averaged over the same time step for
3 nopinone, the sum of methacrolein and methyl vinyl ketone, propionic acid and methyl ethyl ketone.
4 Error bars correspond to the 1σ uncertainties of TD-GC/MS measurements. Error bars correspond to
5 the 1σ uncertainties of TD-GC/MS measurements.

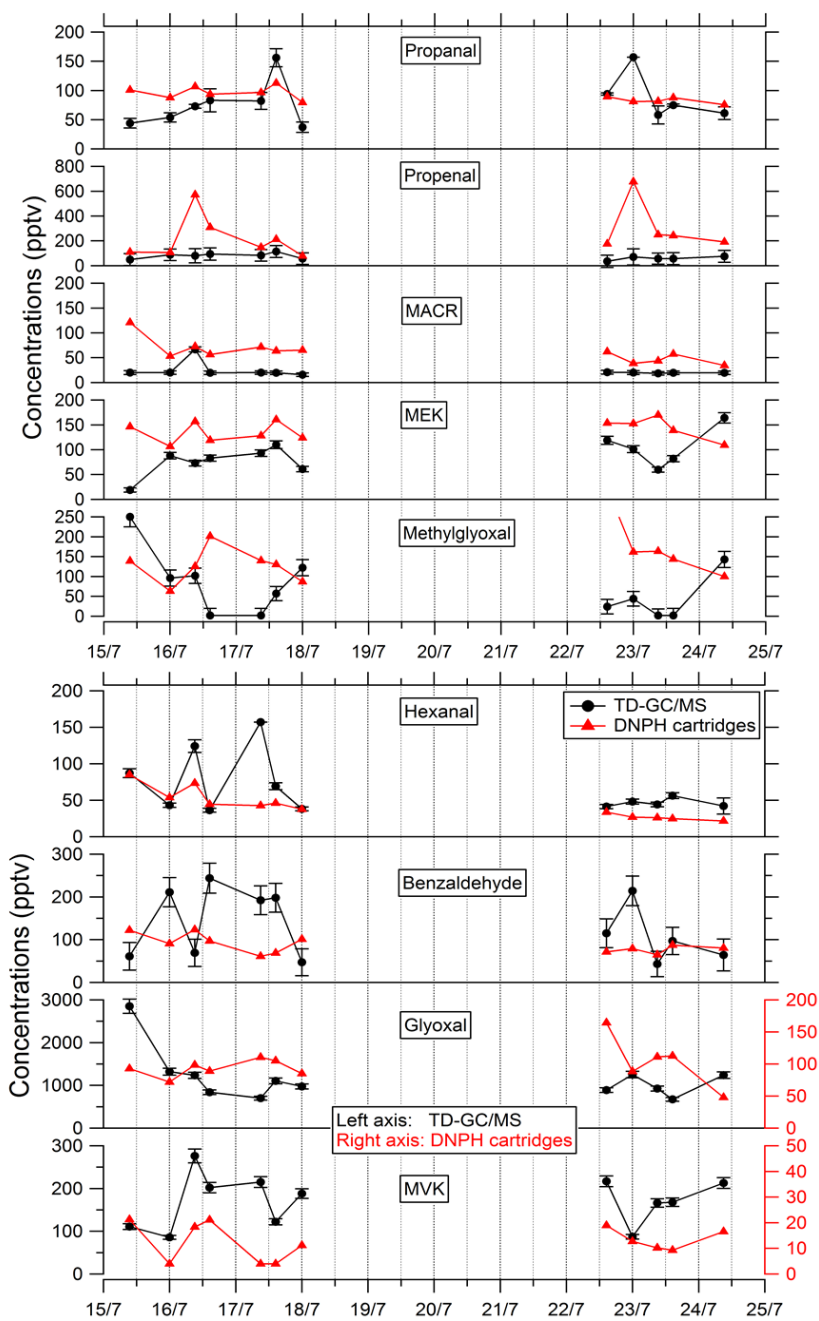
6



1

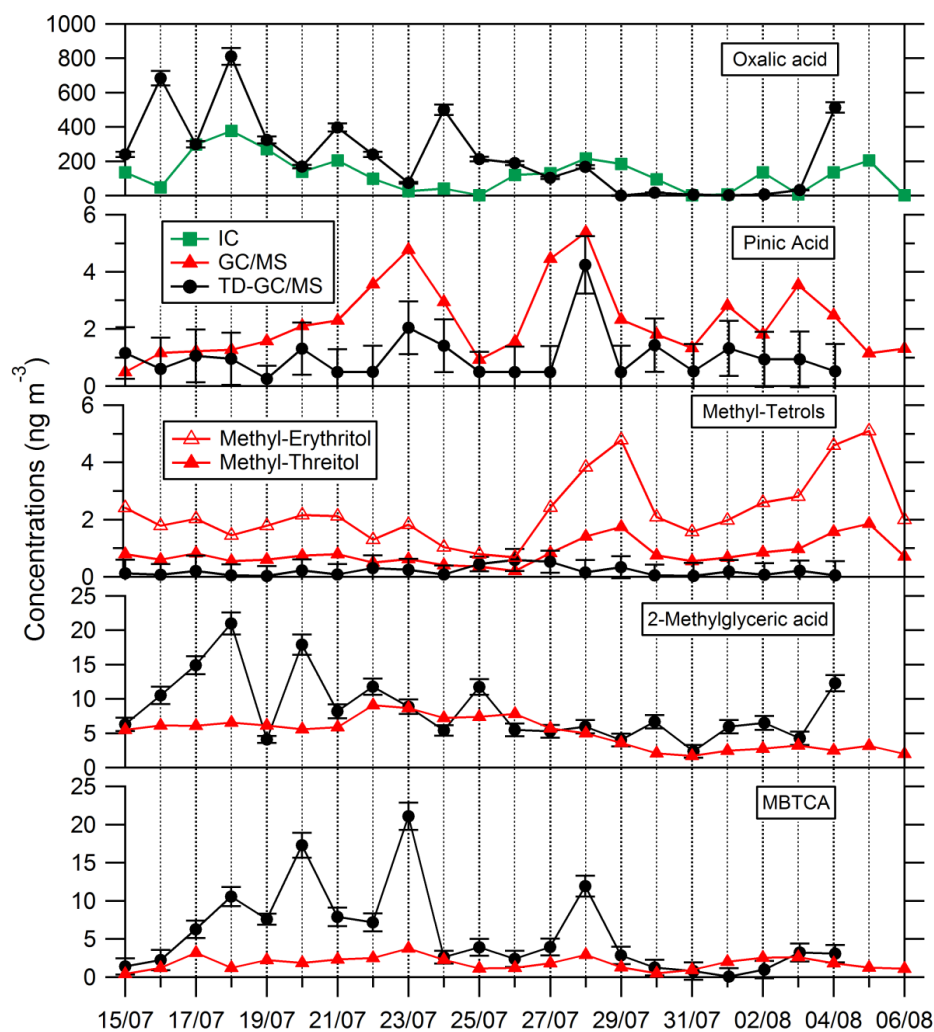
2 Figure 5 : Comparison of ATD-GC-MS data with GC/FID/MS data averaged over the same time step for
3 methyl vinyl ketone and 2-hexanone. Error bars correspond to the 1σ uncertainties of TD-GC/MS
4 measurements. Error bars correspond to the 1σ uncertainties of TD-GC/MS measurements.

5



1

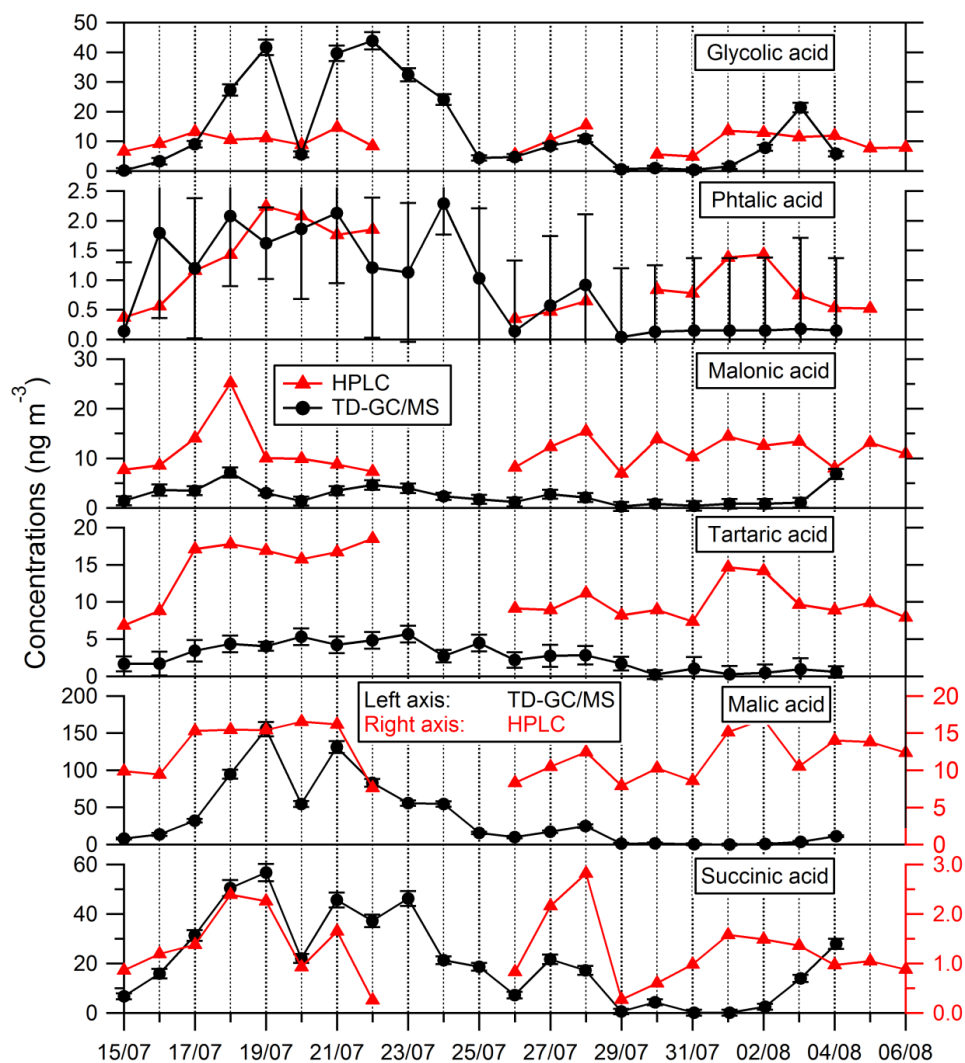
2 Figure 6 : Comparison of ATD-GC-MS data with DNP cartridges analysis for 9 OVOCs. Error bars
3 correspond to the 1σ uncertainties of TD-GC/MS measurements. Error bars correspond to the 1σ
4 uncertainties of TD-GC/MS measurements.



1

2 Figure 7 : Comparison of ATD-GC-MS data with ion chromatography and GC/MS analysis for particulate
3 oxalic acid, pinic acid, methyl tetrols, 2-methylglyceric acid and MBTCA (3-Methyl-1,2,3-tricarboxylic
4 acid). Error bars correspond to the 1σ uncertainties of TD-GC/MS measurements. Error bars
5 correspond to the 1σ uncertainties of TD-GC/MS measurements.

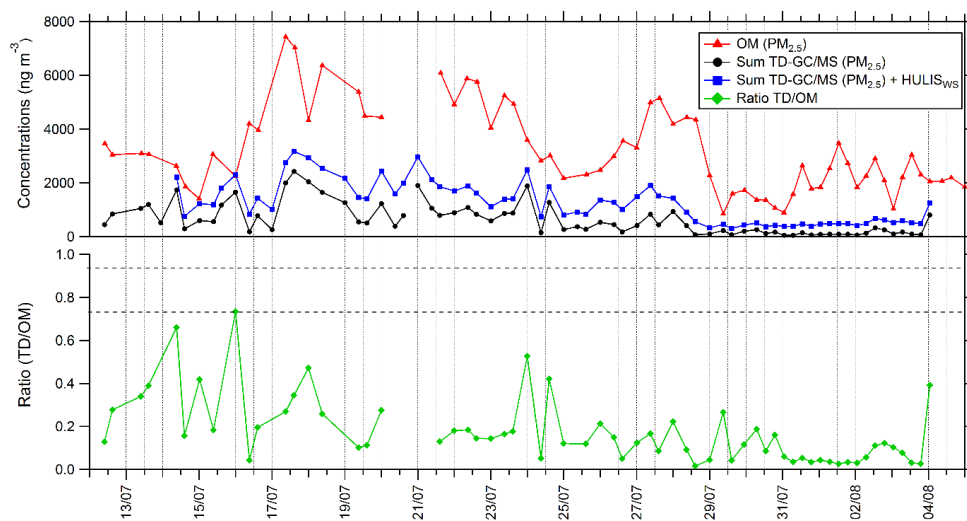
6



1

2 Figure 8: Comparison of ATD-GC-MS data with HPLC analysis for particulate glycolic acid, phthalic acid,
3 malonic acid, tartaric acid, malic acid and succinic acid. Error bars correspond to the 1σ uncertainties
4 of TD-GC/MS measurements. Error bars correspond to the 1σ uncertainties of TD-GC/MS
5 measurements.

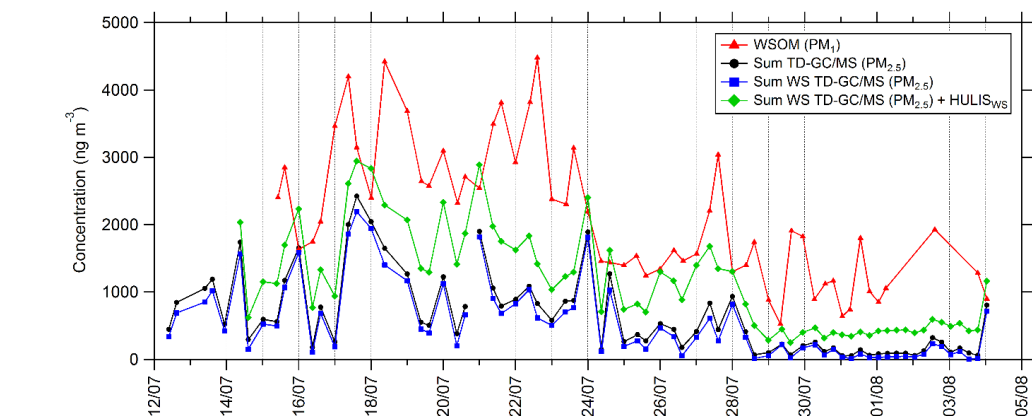
6



1

2 Figure 9: Time series of organic matter in $\text{PM}_{2.5}$ (red line), total sum of $\text{PM}_{2.5}$ from TD-GC/MS analysis
3 (black line), total sum of $\text{PM}_{2.5}$ from TD-GC/MS analysis and water soluble HULIS analysis (blue line),
4 and ratio of these two measurements (green line).

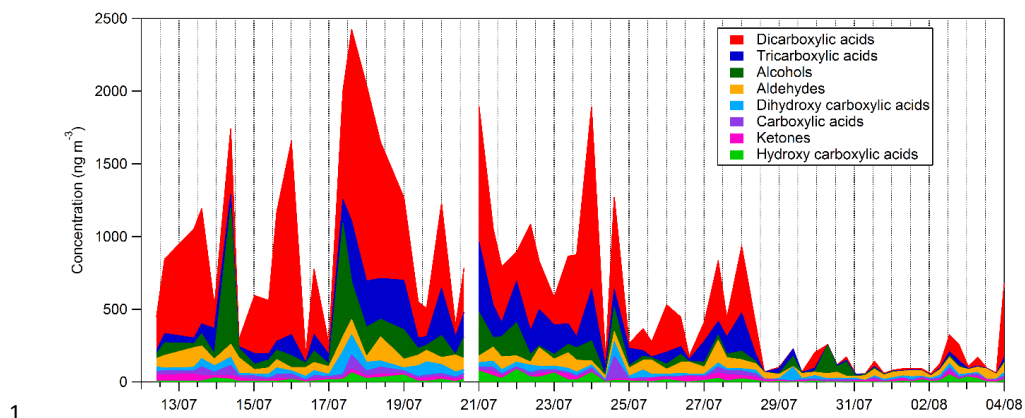
5



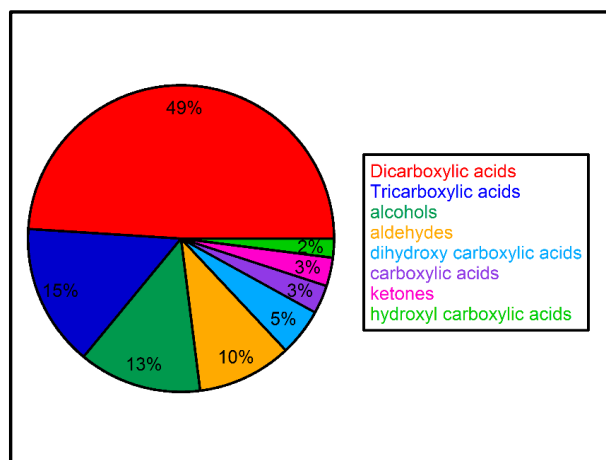
1

2 Figure 10: Time series of PM₁ water soluble organic matter (WSOM; red line), total sum of PM_{2.5}
3 measured by TD-GC/MS (black line), total sum of compounds measured by TD-GC/MS and having
4 henry's law constant higher than 10⁴ M atm⁻¹ measured by TD-GC/MS (WS TD-GC/MS, blue line), and
5 total sum of water soluble compounds measured by TD-GC/MS and water soluble HULIS (green line).

6



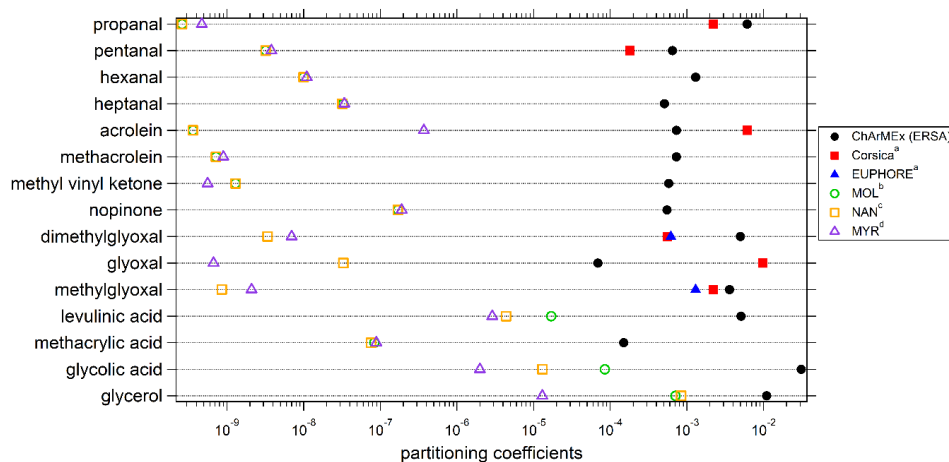
1
2 Figure 11: Time series of the composition of the sum of all compounds concentrations measured by
3 TD-GC/MS.
4



1

2 Figure 12: Campaign averaged relative composition of the sum of all compounds measured by TD-
3 GC/MS in the organic aerosol phase (hydroxyl-carboxylic acid-light green area, ketone-pink area,
4 carboxylic acid-purple area, dihydroxy carboxylic acid-light blue area, aldehyde-orange area, alcohol-
5 dark green area, tricarboxylic acid-dark blue area, dicarboxylic acid-red area).

6



1

2 ^a Rossignol et al., 2016; ^b Moller et al., 2008 (coupled with Nannoolal et al. (2004) method for boiling point determination); ^c Nannoolal et
3 al., 2008 (coupled with Nannoolal et al. (2004) method for boiling point determination); ^d Myrdal and Yalkowsky, 1997 (coupled with
4 Nannoolal et al. (2004) method for boiling point determination)

5 Figure 13: Experimental and theoretical partitioning coefficients determined for this study and
6 compared to previous field and chamber campaigns.